People's Democratic Republic of Algeria
Ministry of Higher Education and Scientific Research
University M'Hamed BOUGARA – Boumerdès

Institute of Electrical and Electronic Engineering
Department of Electronics

Project Report Presented in Partial Fulfilment of
the Requirements of the Degree of

MASTER

In **Telecommunication**

Option**: Telecommunication**

Title:

Design and analysis of compact MIMO antennas for wireless applications

Presented by:

- **Alla Hicham**
- **Naab Anes**

Supervisor:

Dr. K djafri

Registration Number…...../2021

Acknowledgements

First and foremost, we are thankful to Allah, the most gracious, the most merciful for helping us to complete this modest work. It is our belief in him that guided us through the hardest times when it seemed impossible to go on.

Secondly, we would like to express our deepest gratitude to our supervisor “Dr. K Djafri” for her help, guidance, patience, motivation and support.

Her guidance helped us in all the time of research and writing of this thesis. I could not have imagined having a better advisor and mentor for my master study.

Finally, we would like to thank all IGEE teachers and workers.

Dedication

This dedication is for my family, which was, is, and will be the greatest treasure I will have ever. To my parents, Father Alla Nadir and Mother Kheira brinis, for making me the person I am and supporting me all the possible ways. Words cannot describe my love and appreciation for you.

To my brother, the beloved Abdenacer, I wish you a long, happy and successful life.

To my childhood and company friends B. Rachida, H. Hicham, B. Malik, S. Aymen, N. Anes and G. Djawed, we have spent great moments and share many memories with each other, I hope our friendship lasts forever.

To all my family members, particularly, Youssra, Madjid, Rachid and Yacine, I wish you success and happiness in your lives.

ALLA Hicham

I would like to dedicate this work to

my beloved parents, my family and friends.

NAAB Anes

Abstract

In this work, two configurations of a slotted cup-shaped antenna element are proposed to cover the 3.5GHz WiMAX application. The antenna element geometry consists of cup-shaped radiator loaded with two open ended slots to create a band notch at 4.27GHz. An operating bandwidth of 2.9 GHz to 4.2 GHz with inter-port isolation, $S_{21} < -20\,dB$ for pattern diversity configuration, and 3 GHz to 4 GHz with $S_{21} < -22\,dB$ in spatial diversity configuration are achieved. The footprints of the antenna configurations are 48×48 and 29×44 mm^2. The proposed MIMO configurations are simulated using CST software, fabricated and experimentally validated. The designed antenna configurations cover widely the 3.5 GHz intended application and compact.

Table of Contents

List of Abbreviations

MPA	Microstrip Patch Antenna
PCB	Printed Circuit Board
MMICs	Microwave Monolithic Integrate Circuits
VSWR	Voltage Standing Wave Ratio
PIFA	Planar Inverted Frequency Antenna
DGS	Defected Ground Structure
BPSK	Binary Phase Shift keying
QAM	Quadrature Amplitude modulation
2D	Two-Dimensional
3D	Three-Dimensional
CST	Computer Simulation Technology
FR-4	Flame Resistant 4
MIMO	Multiple Input Multiple Output
SISO	Single Input Single Output
SNR	Signal to Noise Ratio
WiMAX	Worldwide Interoperability for Microwave Access
S_{11}	Return Loss
S_{21}	The isolation
VNA	Vector Network Analyzer
SMA	Subminiature Version A
RFID	Radio Frequency Identification

List of Figures

List of Tables

General Introduction

Wireless communication technology transmits information over the air using electromagnetic waves like IR (Infrared), RF (Radio Frequency), satellite, etc. For example, GPS, Wi-Fi, satellite television, wireless computer parts, wireless phones that include 3G and 4G networks, and Bluetooth. Telecommunication these days is mostly wireless. It involves transmission of information without wires, cables or any other electrical conductors within a shorter distance or across the globe. Wireless communications are growing to new heights because of its huge business benefits. Wireless technology offers speed, flexibility, and network efficiency. It has become a powerful tool for tech-savvy generation as it facilitates easy information sharing and boosts productivity[1]. Multiple input multiple output (MIMO) is the key technology in this era leading to the rapid development of wireless communication systems. MIMO is a technique which deploys multiple antennas at input and output terminals of wireless communication systems. MIMO also helps in the reduction of multipath fading thus increasing the performance of the system [2]. The major problem in designing MIMO antenna system is the electromagnetic isolation between various antenna elements taking into consideration the availability of limited space [3]

In this work, two diversity antenna configurations of two elements, i.e. spatial and pattern that are of a cup-shaped patch antenna, are studied. The cup-shaped radiating patch is chosen for its large operating bandwidth. The bandwidth is reduced by cutting two symmetrical open slots to create a notch at 4.27GHz. The isolation in spatial diversity configuration is enhanced by placing two antenna elements in coplanar manner with a distance of 2 mm between the two radiating elements and using a rectangular shaped decoupling stub. In pattern diversity configuration the isolation between the two orthogonal antenna elements is enhanced by using a diagonal T-shaped metallic stub and loading two rectangular slots in the antenna ground plane. The single antenna element and both diversity configurations are designed and analyzed by using a full wave simulator CST.

The report includes three main chapters and it is organized as follows:

Chapter 1 presents an overview on Microstrip Patch Antenna and introduces MIMO antenna systems including basic parameters, types, applications and techniques of isolation.

Chapter 2 gives the steps of designing the cup-shaped microstrip patch antenna operating in the frequency band 3 GHz to 4 GHz, starting from a semi-circular patch ending by open-end slotted cup-shaped radiating patch. Three intermediate structures are considered and theirs return losses over the considered range of frequency are simulated and analyzed.

Chapter 3, the detailed analysis of the proposed MIMO configurations, spatial diversity and pattern diversity, is provided. In addition, an extensive parametric study for both proposed structures is carried out in order to have a better understanding of the operating mechanism.

A conclusion is presented at the end of the report.

CHAPTER 1

Introduction to Microstrip Patch Antennas and Multiple Input-Multiple Output (MIMO) System

1.1 Introduction to Microstrip Patch Antennas

1.1.1 Introduction

The microstrip patch antenna MPA is one of the structures that are widely used because of its low cost, ease of fabrication and implementation. In its simplest form, a MPA consists of a metallic patch placed on a dielectric material and supported by a ground plane. It can be easily fabricated on printed circuit board. The mostly used design is shown the Figure 1.1.

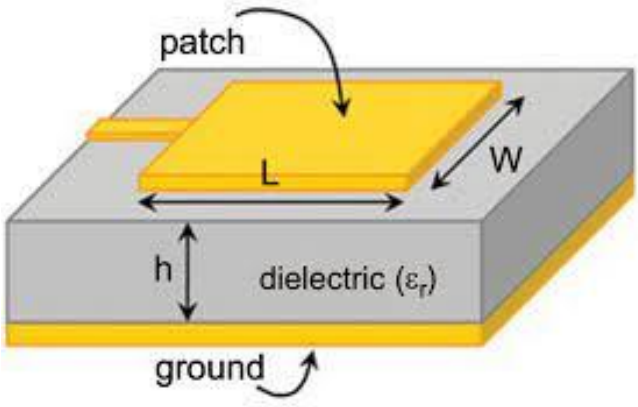

Figure 1. 1 : Microstrip Patch Antenna Configuration

- **The History of Microstrip Antennas**

Microstrip antennas were first developed in the 1950's. However, this concept had to wait for about 20 years to be realized after the development of the printed circuit board (PCB) technology in the 1970's. Since then, microstrip antennas are the most common types of antennas with wide range of applications due to their apparent advantage of light weight, low profile, low cost, planar configuration, ease of conformal, superior potability, suitable for array with the simple way of fabrication and integration with microwave monolithic integrate circuits (MMICs). They have been widely engaged for the civilian and military applications such as radio-frequency identification (RFID), television, multiple input multiple output (MIMO) systems [4].

1.1.2 General Description

MPAs consist of dielectric material known as substrate that have a rectangular form and two conductors placed on the top and bottom surface. The metallic patch which is the radiating element is placed on the top of the dielectric material. To give supply to the microstrip antenna a transmission line is connected to the patch to excite it. On the bottom

surface the placed conductor is known as ground. The radiating conductor can be designed in various shapes based on the desired characteristics and applications.

1.1.2.a Conductiong Layer

The common materials used for conducting surfaces are copper foil or copper foil plated with corrosion resistant metals like gold, tin, and nickel. These metals are the three main choices because of their low resistivity, resistant to oxidation, solderable, and adhere well to substrate [5].

The patch consists of a very thin metallic strip ($t \ll \lambda_0$ where, λ_0 is the free-space wavelength) placed a small fraction of wavelength (h) above the ground plane. The microstrip patch is designed so its maximum pattern is normal to the patch. This is accomplished by properly choosing the mode of excitation beneath the patch [6].

1.1.2.b Dielectric Substrate

The substrate is a base or a container on which the antenna is fabricated. it is needed for the mechanical support. To provide this support it should consist of a dielectric material. This middle layer works as an isolator, and it is considered as the main component of the microstrip structure. The selection of this isolator plays a big role to achieve best results. There are numerous substrates that can be used for the design of the microstrip antennas. Their dielectric constants are usually in the range of $2.2 \leq \varepsilon r \leq 12$. Thick substrates whose dielectric constant belongs to the lower end of the range are advantageous since they provide better efficiency, larger bandwidth, loosely bound fields for radiation into space [6]. This layer has a major effect on the bandwidth because any increase in the dielectric constant causes a decrease in the resonant frequency as well as the bandwidth.

1.1.3 Microstrip Antenna Configurations

Due to the early expansion of the microstrip antennas, several designs and configurations have been created and tested to reach the desired performance. Some of the common forms are rectangle, triangle, and circular. One of the common ways to improve the antenna performance is to combine many structures. Figure 1.2 below shows some of the common shapes that a patch can take.

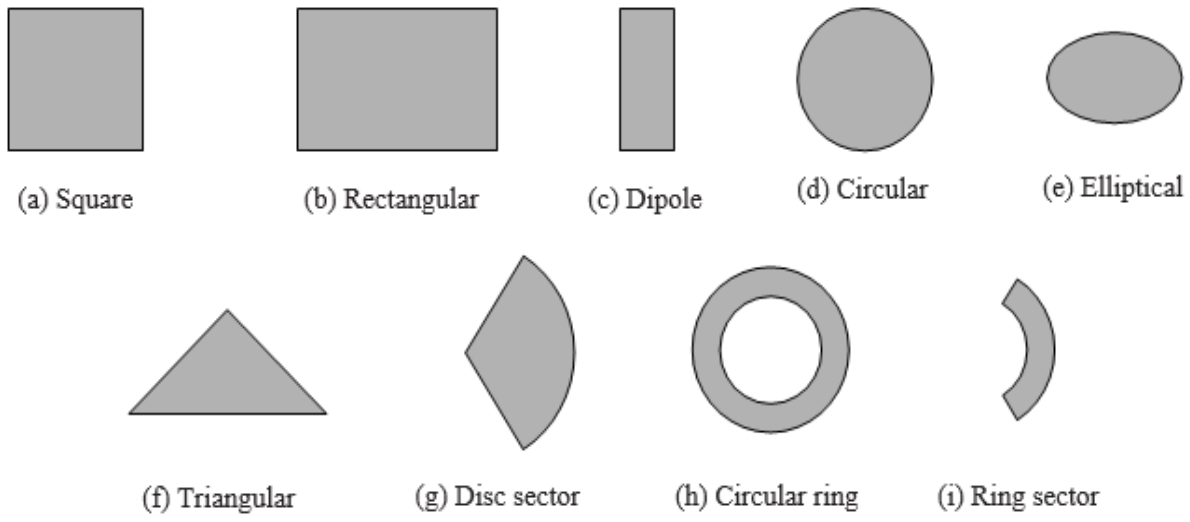

Figure 1. 2: Common Shapes of Microstrip Patch Antennas [6].

1.1.4 Basic Parameters

Before designing any antenna, several antenna characteristics should be taken into consideration. Generally, they are identified by input impedance, return loss, directivity, radiation pattern, and bandwidth. Some of the basic parameters are described:

1.1.4.a Input Impedance

Z_{in} is the impedance presented by an antenna at its terminals, or the ratio of the voltage to current at a pair of terminals, or the ratio of the appropriate components of the electric to magnetic fields at a certain point [6]. It's represented as follows:

$$Z_{in} = R_{in} + jX_{in} \tag{1.1}$$

Where R_{in} is the real part of the input impedance, and X_{in} is the imaginary part.

1.1.4.b Return Loss S_{11}

Testing any antenna requires some essential parameters such as the return loss, which deals basically with how perfectly the impedance matching between the two ports is done. In simple words it represents the ratio between the reflected power (P_r) and the incident power (P_i). It is defined as :

$$RL(dB) = -10log\left(\frac{P_r}{P_{in}}\right) \tag{1.2}$$

S_{11} below -10dB means at least 90% input power is delivered to the antenna and the reflected power is less than 10%. This value is sufficient for many applications. The minimum frequency given by the return loss is taken as resonant frequency of the device [7].

1.1.4.c Voltage Standing Wave Ratio (VSWR)

VSWR is a numerical value that describes how well the antenna impedance is matched to the feedline impedance. This numerical quantity is always real and positive. VSWR is a function of the reflection coefficient, equation (1.3) defines VSWR [8]:

$$VSWR = \frac{1 + |\Gamma|}{1 - |\Gamma|} \tag{1.3}$$

VSWR can also be written in terms of Vmax and Vmin as follows:

$$VSWR = \frac{Vmax}{Vmin} = \frac{1 + \rho}{1 - \rho} \tag{1.4}$$

Where Γ is the reflection coefficient or S11 and ρ is the magnitude of Γ.

1.1.4.d Directivity

The directivity of an antenna is defined as the ratio of the radiation intensity *U* in a given direction from the antenna to the radiation intensity averaged over all directions. The average radiation intensity is equal to the total power P_r radiated by antenna divided by 4π. The direction of nonisotropic source is equal to the ratio of the radiation intensity *U* in a given direction over the radiation intensity U_0 of an isotropic source [9]. In mathematical form, it can be written as:

$$D = \frac{U}{U_0} = \frac{4 \times \pi \times U}{P_r} \tag{1.5}$$

1.1.4.e Gain and Efficiency

Antenna gain is defined as antenna directivity times a factor representing the radiation efficiency, this efficiency is defined as the ratio of the radiated power (P_r) to the input power (Pi). The input power is transformed into radiated power and surface wave power while a small portion is dissipated due to conductor and dielectric losses of the materials used [10].

1.1.4.f Bandwidth

The bandwidth of an antenna is defined as the range of frequencies within which the performance of the antenna with respect to some characteristics conforms to a specified standard. Since the antenna characteristics (input impedance, gain, polarization…) do not always vary in the same manner, it is possible to consider several definitions of the antenna bandwidth, impedance bandwidth, directivity bandwidth, polarization bandwidth, and efficiency bandwidth. Directivity and efficiency are often combined as gain bandwidth [11].

1.1.4.g Radiation Pattern

Radiation pattern describes the strength of the radiated field distribution as a function of space coordinates. In most cases, it is represented in 3D or 2D in the far-field region and usually in polar format [6].

1.1.5 Feeding Techniques

MPA feeding techniques can be classified into two main categories: direct and indirect contact. Direct contact is where the power is directly inserted to the radiating patch, microstrip line and coaxial line are the most common ones. Whereas, indirect contact is where the power is fed via coupling between the conductor sheet and the microstrip line, aperture coupling and proximity coupling are the well-known among this category.

a) **Microstrip Line Feed:** a strip directly connected to the patch. the strip impedance may differ from that of the patch, one of the techniques to match both impedances is to add an inset cut to the patch to achieve a succeful feeding.
b) **Coaxial Feed:** from the general fact that the coaxial cable has inner and outer conductor, the inner is connected to the patch through the dielectric substrate while the outer one is connected to the ground plane. The input impedance can be controlled from changing the position of the feed.
c) **Aperture Coupled Feed:** This technique adopts a different configuration where the radiation patch is totally separated from the feed line by the ground plane with an aperture to provide the power transmission.
d) **Proximity Coupled Feed**: like the previous technique, there are also two substrates. The microstrip feed line lies between the two substrates whereas the radiating patch is placed on the upper substrate. Figure 1.3 below shows all the mentioned techniques

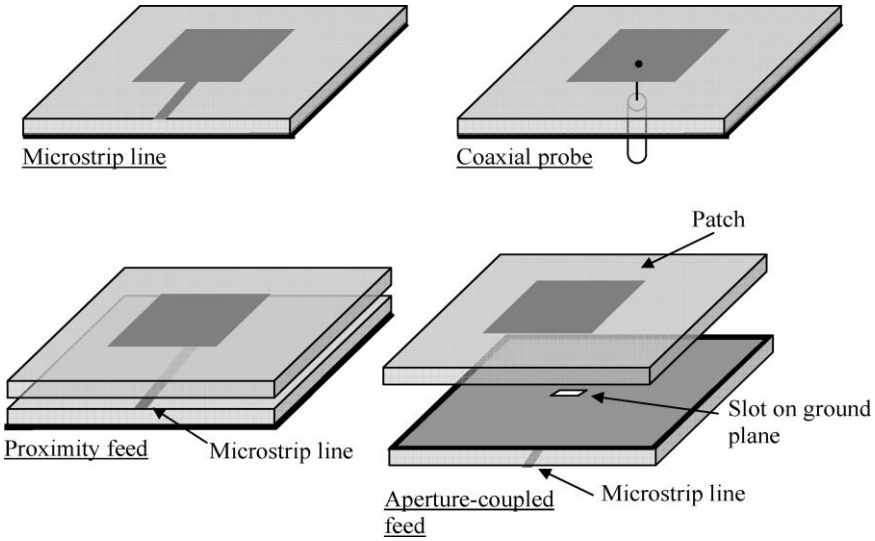

Figure 1. 3: Microstrip Patch Antennas feeding techniques [12]

1.2Introduction to Multiple Input-Multiple Output Systems

1.2.1 Introduction

Multiple input, Multiple output (MIMO) systems have been one of the most active areas of research and development in the broad field of the wireless communications. These systems enhance the data transferring rate and reduce the probability of error by taking advantage of multiplexing and diversity, respectively [13]. However, MIMO systems face some challenges such as mutual coupling, which affects the antenna characteristics by reducing the efficiency, increasing the correlation and coupling power and reducing the radiated power [14]. There are many considerable works that have been conducted to deal with such challenges. Among the available solutions is increasing the distance between antennas which is undesirable because this procedure will increase the system's overall size which is not functional for most mobile applications. To solve this problem many technologies have been invented to keep the size within the suitable dimensions. In this section, we will see some generalities about MIMO antenna systems

1.2.2 Diversity Techniques

1.2.2.a Space Diversity

Two closely coupled antenna radiators can be de-correlated using the space variation. The space variation is the key of this approach to achieve low mutual coupling. all types of MIMO antennas like conventional and non-conventional shaped monopole, dipole, planar

inverted frequency (PIFA) etc, use the space diversity. The mutual coupling in this technique is studied in terms of ground and patches, separation and orientation of the radiators [15].

1.2.2.b Pattern Diversity

Pattern diversity imposes orthogonality by producing spatially (angularly) disjoint radiation patterns as shown in Figure1.4. This is done by shaping the radiation patterns associated with different ports. External beam-forming can be used to generate pattern diversity [16].

1.2.3 Mutual Coupling Reduction Techniques

As stated before any MIMO antenna system should be constructed in a limited space using a suitable isolation technique to minimize the coupling effect and to have a compacted design for the specific application. Many techniques were developed for this task and some of them were used in this report work. Placing the system radiating elements in an orthogonal orientation can reduce the mutual coupling. Slots are one of the key methods for the decoupling purpose, they can take many shapes depending on the needed applications. They are mostly etched on the ground plane to reduce the spacing between the radiating elements which results in the reduction of the correlation factor. In addition, stubs also are widely used for the isolation task; they can have many shapes and positions. Stubs and slots can be combined in same system for better results. Furthermore, the defected ground structure (DGS) is also a wildly adopted technique. This method uses slits placed on the ground plane. It is functional for the reduction of the antenna size and helps suppress the coupling fields between the MIMO elements.

1.2.4 MIMO Applications

1.2.4.a Data Rate Extension

MIMO with low bandwidth and high spectral efficiency solves the problem of high speed and low speed users. In MIMO 1 Gbps data rate is achieved with 20 MHz bandwidth only. MIMO with different modulation like binary phase shift keying (BPSK), quadrature phase shift keying (QPSK), and quadrature amplitude modulation (QAM), offers variable data rates [15].

1.2.4.b Power Saving

Unlike other systems like SISO, MIMO does not consume much power. Therefore, it is suitable for wireless applications [15].

1.2.4.c Capacity Enhancement

Capacity of MIMO is very high and is not dependent completely on the bandwidth. It increases linearly. The Capacity is affected by the signal to noise ratio(SNR) [15] .

1.2.5 Conclusion

In this chapter, MPAs where introduced and described along with feeding techniques, fundamental parameters and methods of analysis. Antenna parameters such as radiation pattern, return loss, and gain take a huge amount of interest when analyzing the antenna performance. MIMO antenna systems were also presented. The fundamental techniques such as isolation to achieve better MIMO antenna performance were also reviewed.

CHAPTER 2

Design and Analysis of Cup-Shaped Microstrip Patch Antenna

2.1 Introduction

In this chapter, the study and design of semi-circular based microstrip patch antenna is presented. The proposed design evolution stages are also investigated. The design procedure starts with a simple semi-circular shaped patch antenna. Then, to cover the 3.48 GHz, a rectangular shaped patch is attached to the semicircular structure and hence a cup-shaped patch is obtained. Finally, to two open slots are loaded to the cup-shaped structure to create a notch at 4.27 GHz and limit the frequency bandwidth. The return loss, current distribution and radiation patterns are simulated using a full wave simulator CST (computer simulation technology).

2.2 Design of Cup-shaped Microstrip Single Patch Antenna

2.2.1 Antenna Structure

In order to obtain the proposed antenna, a semi-circular patch of radius R is designed then H-shaped patch is added to it. The resulted patch is fed by a 50-Ω microstrip feedline and printed on the top side of FR-4 substrate with relative permittivity 4.3 loss tangent 0.017 and width 1.6 mm. On the bottom side of the substrate is a partial ground plane with a rectangular shape. The geometric configuration of the proposed antenna is shown in Figure 2.1 and its dimensions are given in Table 2.1.

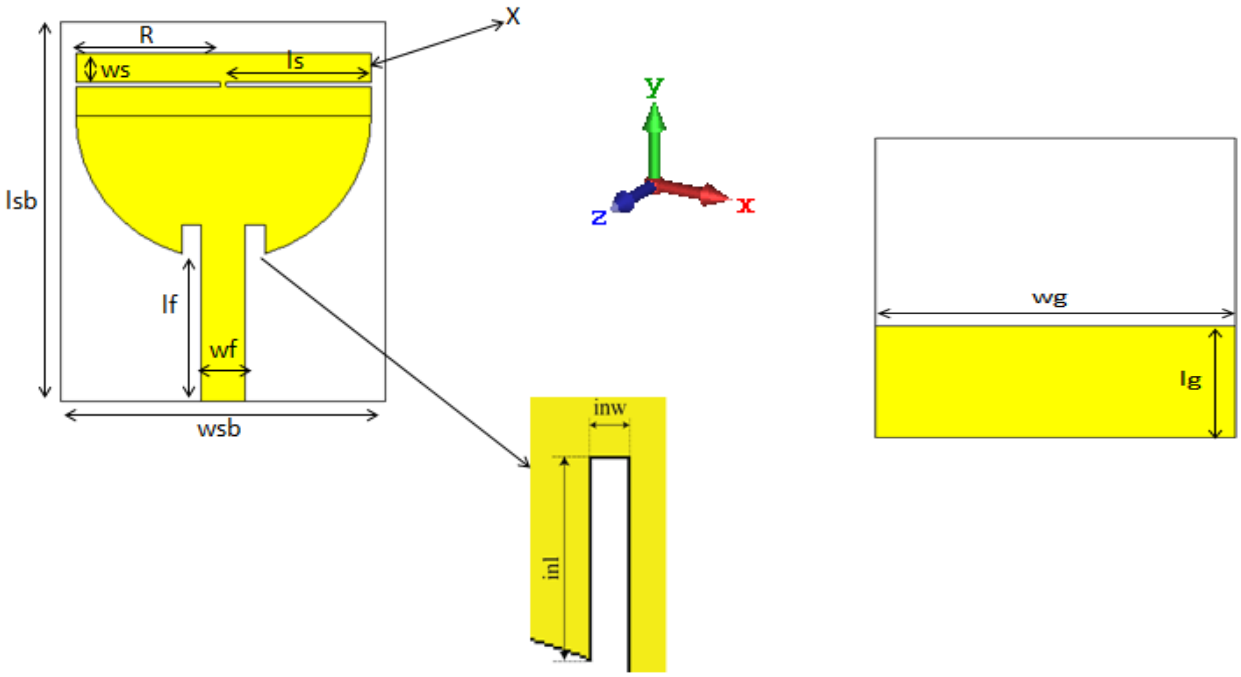

Figure 2. 1: The proposed cup-shaped microstrip patch antenna.

Table 2. 1: Geometric dimensions of the proposed antenna

Parameter	R	X	lf	wf	inl	inw	ls	ws	wg	lg	lsb	wsb
Value (mm)	10	2	10.02	3	2.3	1.3	9.8	0.3	22	9.8	26.32	22

2.2.3 Design Evolution

The initial structure namely Antenna0 is designed and shown in Figure 2.2(a). A finite ground plane of 22×9.8 mm^2 has been printed on back side of the antenna and semi-circular shaped radiator is printed on the front side of the antenna. It can be observed from Figure 2.3 that this structure operates in the frequency band extending from 3.5 to 6.5 GHz. In order to cover the 3.48 GHz WiMAX application, Antenna0 is extended in the y direction by a rectangular patch to obtain the cup-shaped structure namely Antenna1. It can be observed from Figure 2.3 that Antenna1 operates in the frequency band extending from 3 to 6 GHz and covers widely the intended application. Next, two open end-slots are etched from the antenna patch to obtain the proposed antenna (Antenna2). The resulted structure operates in two bands extending from 3 to 4 GHz and 4.5 to 7 GHz. The two slots have created a notch band extending from 4 to 4.5 GHz.

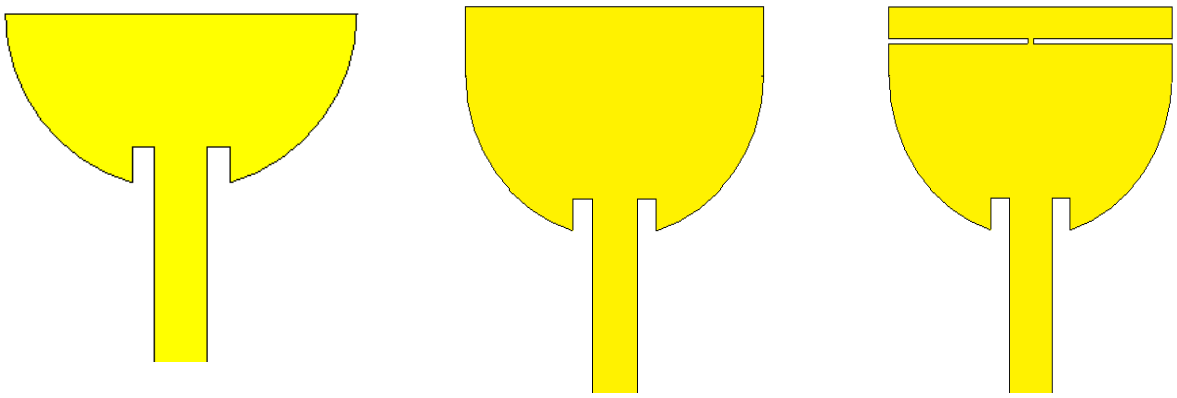

Figure 2. 2: Design evolution (a) Antenna0 (b) Antenna1 (c) Antenna2.

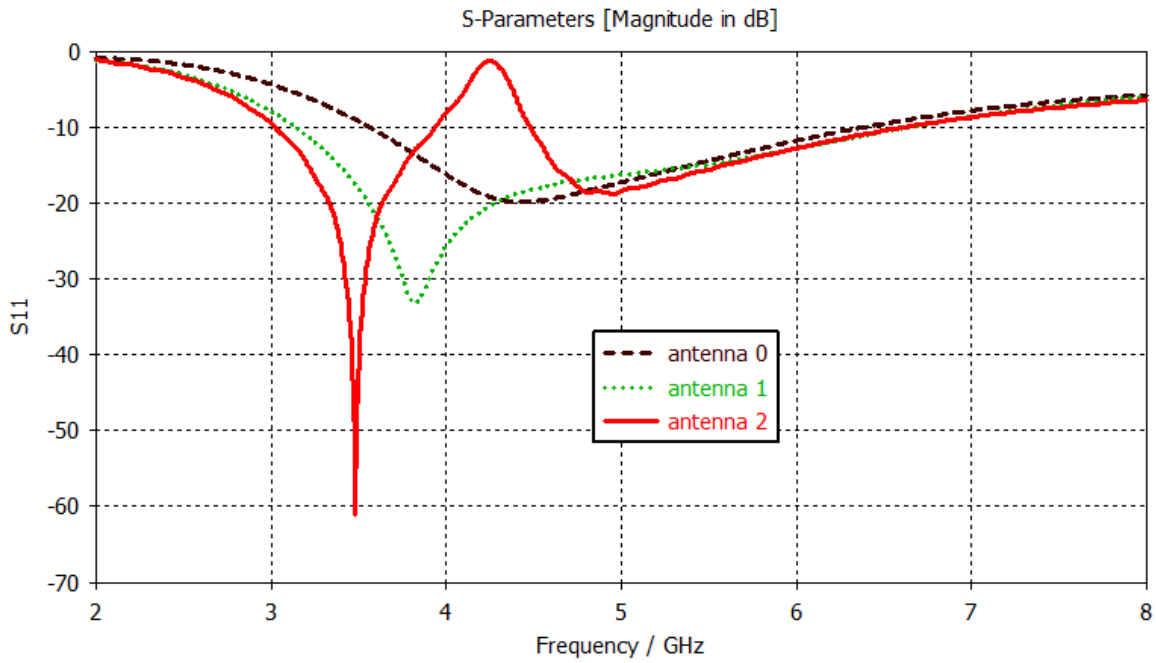

Figure 2. 3: Reflection coefficients for various antennas involved in the design evolution.

2.3 Parametric Study

To study the effect of key geometrical parameters, which affects the antenna performance most, on the antenna reflection coefficient a parametric study is carried out. The simulation are done by changing one parameter at a time while keeping the remaining parameters constants.

The coming section deals with the study of the reflection coefficient response as a function of frequency by varying the slot length.

2.3.1 Effect of Slot Length (ls) on the Return Loss.

Figure 2.4 shows the reflection coefficients for different values of slot length (ls). It can be seen that by increasing the slot length ls from 6.8 mm to 9.8 mm by a step of 1 mm, the notched band shifts toward lower frequencies side. The average length of the slot is $\lambda/4$ at the desired frequency and can be calculated by [17].

$$ls = \frac{c}{4f\sqrt{\varepsilon_{eff}}} \tag{2.1}$$

Where

$$\varepsilon_{eff} = \frac{\varepsilon_r + 1}{2} \tag{2.2}$$

is the effective dielectric constant and *c* is the speed of light.

For Ls = 9.8 mm, the antenna operates in the frequency band 3-4 GHz with best return loss level. Consequently, the value of Ls is taken to be equal to 9.8 mm in the reminder of this chapter.

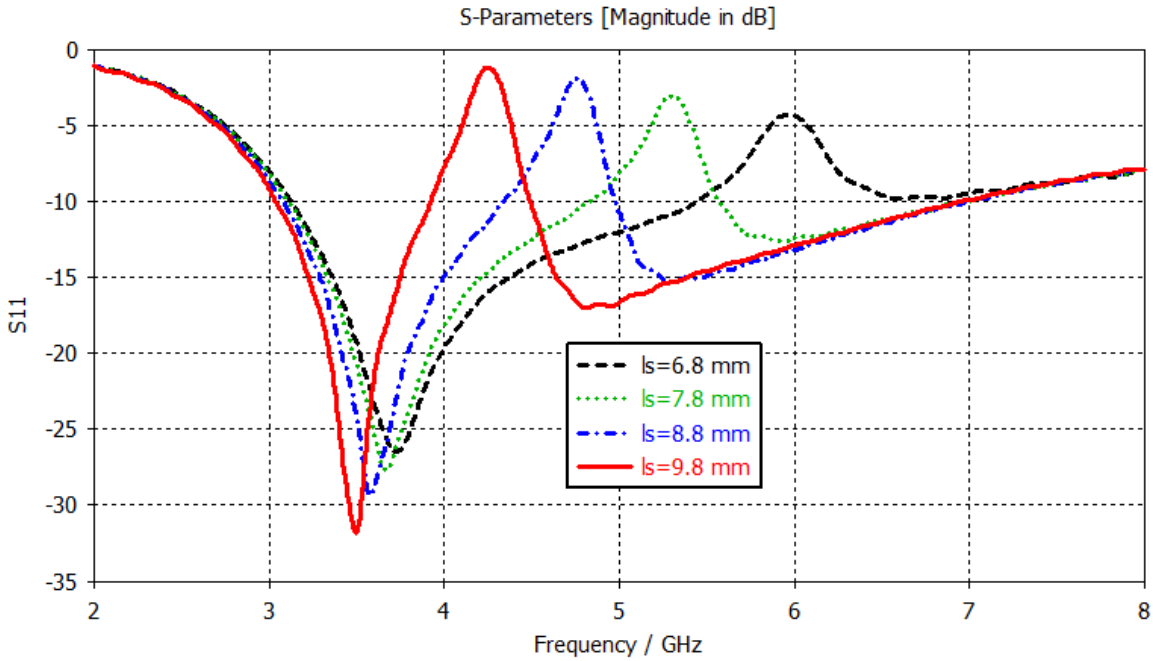

Figure 2. 4: Effect of slot length variation on the return loss.

The upper graph shows the response of reflection coefficient under the variation of slot length Ls.

The microstrip patch antenna is operating at the frequency band of 3-4 GHz , We notice that the optimum response which is the smallest value of S_{11} is obtained when the slot length is Ls = 9.8 mm . It is clearly shown that varying ls affect the notch such that as much as the slot length is decreased the notch is extended.

2.3.2 Effect of Slot Width (ws) on the Return Loss

The effect of the slot width ws on the antenna reflection coefficient is presented in Figure 2.5. It can be observed from the results that as the slot width increases the notched band shifts toward lower frequency side. Moreover, the first operating bandwidth decreases with the increase of ws. Since the main objective of this work is to design an antenna covering

the 3.48 GHz WiMAX band and the first operating band is centered at 3.48 GHz for ws = 0.3 mm,then the considered value of ws is 0.3 mm.

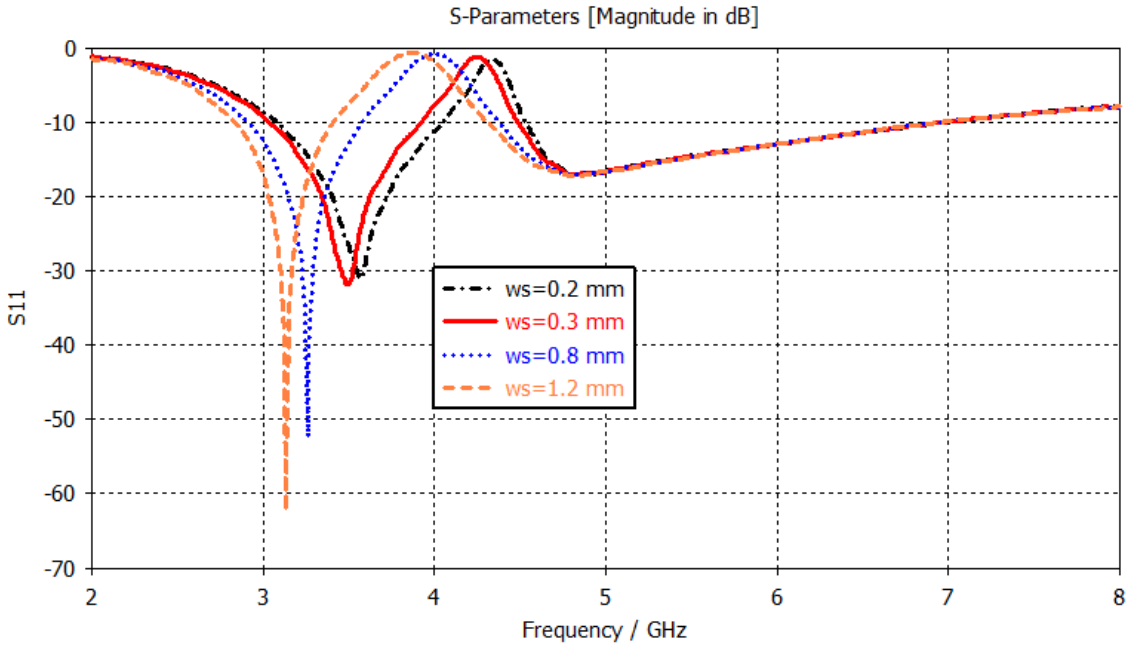

Figure 2. 5: Effect of slot width variation on the return loss.

2.3.3 Effect the length X on the Return Loss

Figure 2.6 shows the simulated reflection coefficients for different values of X. It is clearly seen that by increasing X, increasing the antenna dimension in the y direction, the antenna first operating band moves toward lower frequencies. This is due to the fact that the current path gets lengthened by increasing X and hence decrease the operating frequency band. The first operating band is centered at 3.48GHz for X =2 mm

.

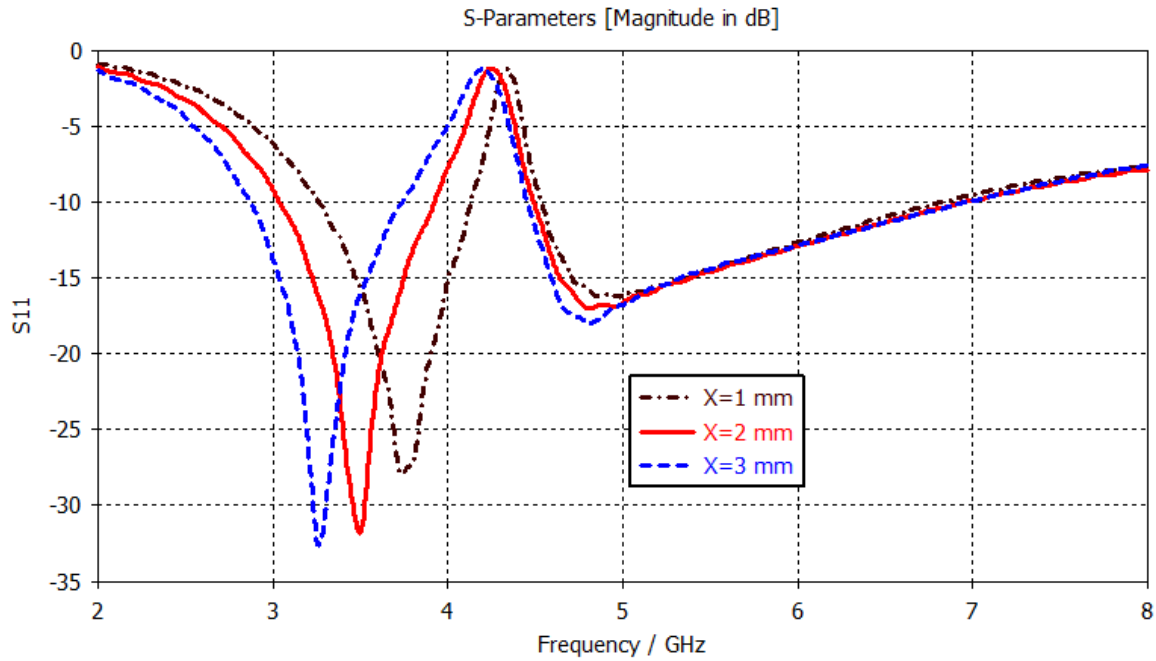

Figure 2.6 :Effect of X variation on the return loss

2.3.4 Effect of the Inset Length (inl) on the Return Loss

To improve the antenna matching, the inset has been introduced. The effect of the inset length on the antenna return loss is depicted in Figure 2.7. It can be concluded from the results that best matching is obtained for inl equals 2.2 mm.

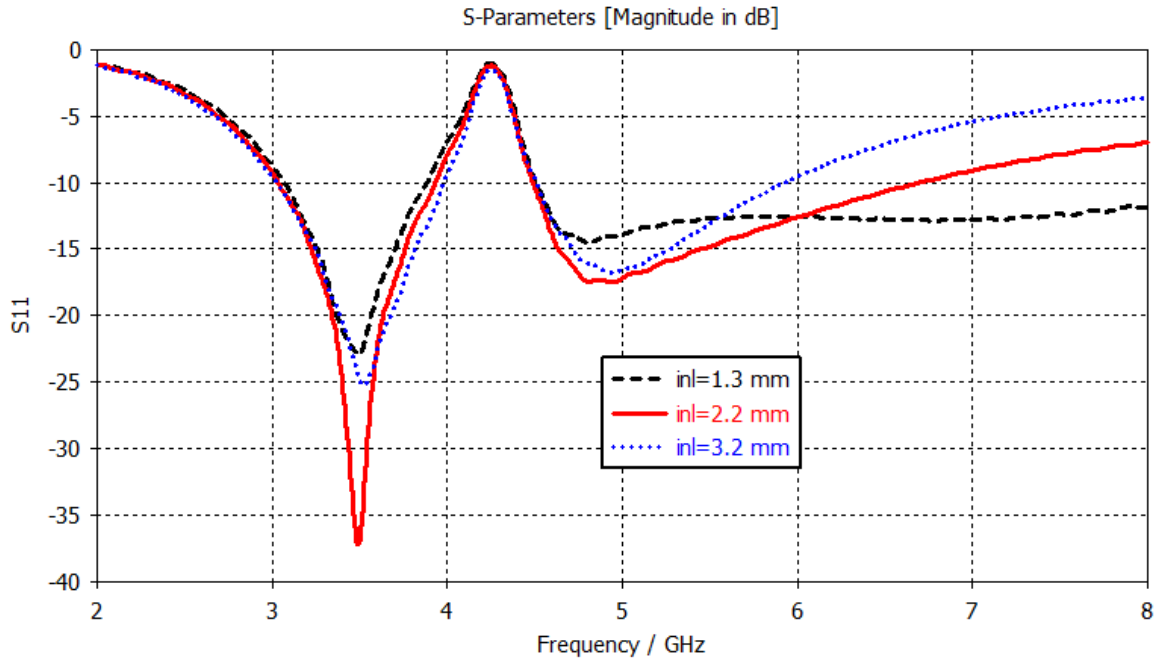

Figure 2. 6: Effect of inset length variation on the return loss.

2.3.5 Inset Width (inw) Effect on the Return Loss

Simulated reflection coefficients for different values of the inset width are presented in Figure 2.8. It is clear from the results that the best matching is achieved for inw =1.3 mm.

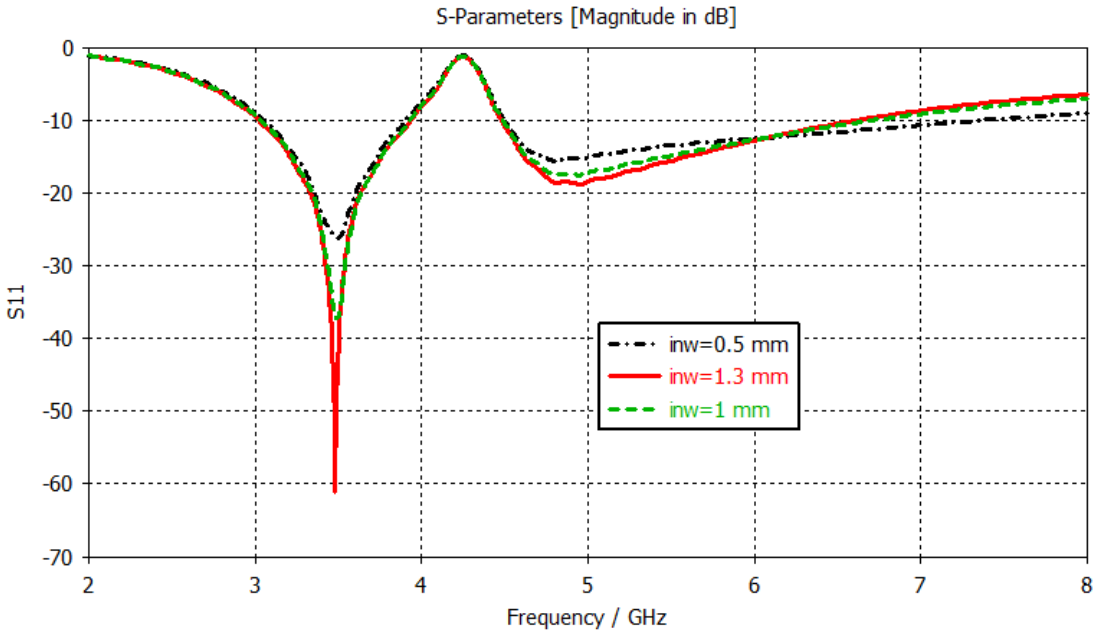

Figure 2. 7: Effect of the inset width variation on the return loss.

2.4 Current Distribution

The simulated current distributions for proposed antenna at the resonant frequency 3.48 GHz and the notched frequency 4.27 GHz are shown in Figure 2.9.

Figure 2.9(a) shows the antenna current distribution at the resonant frequency. It is clear that the surface current distribution is mainly concentrated on semicircular patch as well as the central part of the H-shaped patch, while it is very weak on the radiating patch corners.

It can clearly be seen that the current distribution, at the notched band depicted in Figure 2.9(b) is concentrated at the feedline and the two open-end slots. This demonstrates that the notched band is generated by the pair of slots on the patch.

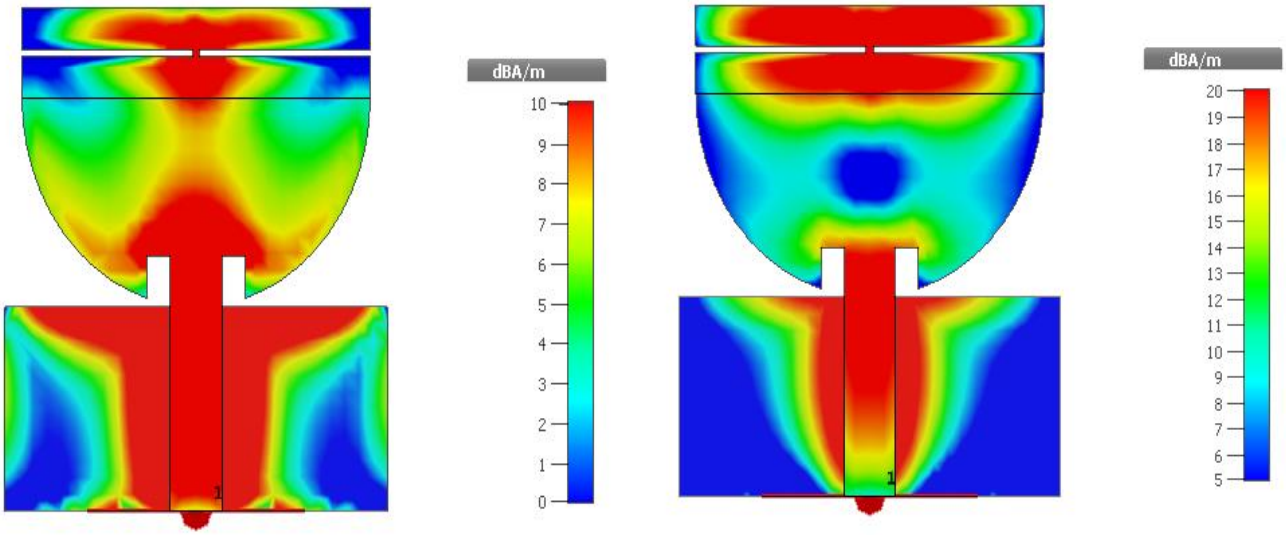

(a) (b)

Figure 2. 8: Simulated current distribution of the proposed structure at (a) the resonant frequency 3.48GHz (b) the notched frequency 4.27GHz.

2.5 Radiation Pattern

The simulated 3D radiation pattern at the resonant frequency is presented in Figure 2.10. It can be seen that the radiation pattern has a form of a doughnut. The E-Plane and H-plane radiation patterns are presented in Figure 2.11. It can be observed from the far-field radiation patterns that the proposed antenna exhibits bidirectional pattern at the resonant frequency 3.48 GHz in E-plane Figure 2.11(a). The radiation pattern results are omnidirectional in H-plane Figure 2.11(b). Also, it can be observed that the peak simulated gain is of 2.48dB.

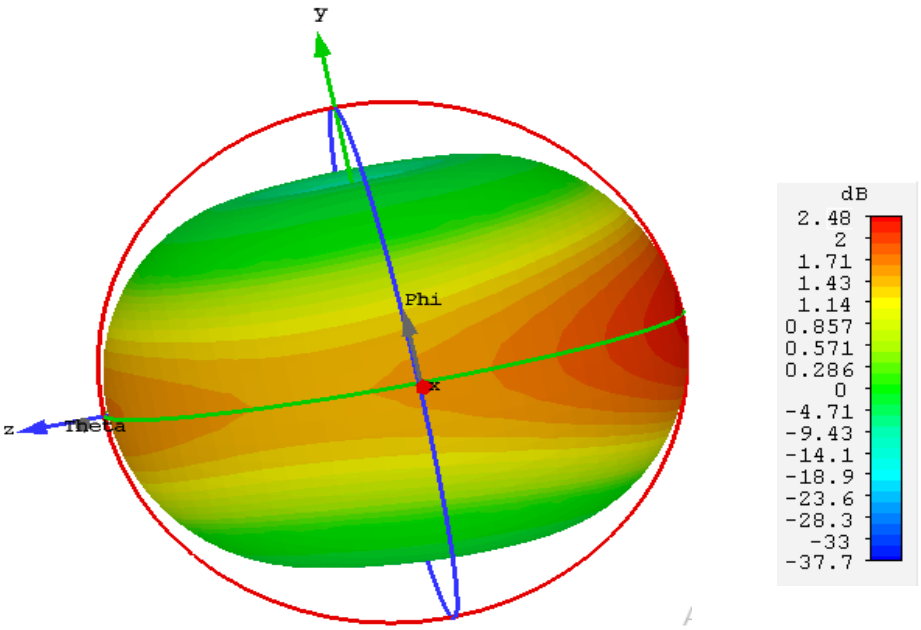

Figure 2. 9: 3D view of the radiation pattern at 3.48 GHz.

It can be seen that at the resonant frequency, the maximum gain is 2.48dB and the antenna exhibits an omnidirectional radiation pattern in the H-plane and dipole-like radiation in the E-plane.

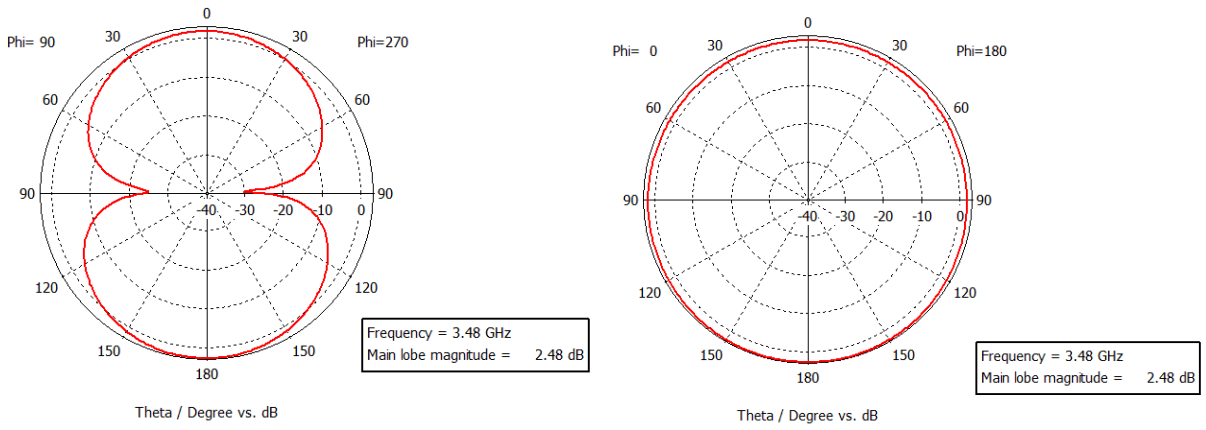

(a) (b)

Figure 2. 10: (a) E-plane and (b) H-plane radiation patterns of the cup-shaped antenna at 3.48 GHz.

2.6 Conclusion

In this chapter, a cup-shaped microstrip patch antenna operating in the frequency band extending from 3 to 4 GHz has been studied and designed. Moreover, the proposed antenna has been loaded by two open-end slots to create a notched band centered at 4.27 GHz. Then, the structure operating mechanism has been investigated by un extensive parametric study and its radiation characteristics in terms of radiation pattern and reflection coefficient have been simulated. The proposed antenna will be used as antenna element in MIMO configurations.

CHAPTER 3

Design and Analysis of Cup-Shaped MIMO Antenna

3.1 Introduction

In this chapter, the study and design of two MIMO configurations will be presented. The proposed designs evolution stages will be also investigated. The slotted cup-shaped patch antenna presented in the previous chapter will be used in both configurations as a basic antenna element. To have a good isolation between the antenna elements two different configurations, pattern and spatial diversity, will be studied and analyzed.

For pattern diversity configuration, two identical antennas are arranged orthogonally to enhance the isolation between the elements 1 and 2. To further reduce the mutual coupling, a T-shaped stub is embedded diagonally in the antenna ground plane. While for spatial diversity case, both patches are placed side-by-side with 2 mm separating distance. To achieve better isolation, a rectangular stub is used and printed in the antenna ground plane. The simulated and measured return losses and radiation patterns of the proposed antennas will be presented and discussed.

3.2 Pattern Diversity Configuration Design

3.2.1 Antenna Structure

For pattern diversity configuration, two identical cup-shaped antenna elements designed in the previous chapter are arranged orthogonally, to improve the isolation with a distance of 13 mm between the centers of the radiating elements. A T-shaped stub is placed diagonally across the substrate and printed in the back side of the substrate to further enhance the isolation. The radiating elements are fed by a 50-Ω microstrip feedlines and printed on the top side of FR-4 substrate with relative permittivity of 4.3, loss tangent 0.017 and width of 1.6 mm. On the bottom side of the substrate is the ground plane and the T-shaped stub. The geometric configuration of the proposed MIMO antenna is shown in Figure 3.1 and its dimensions are given in Table 3.1.

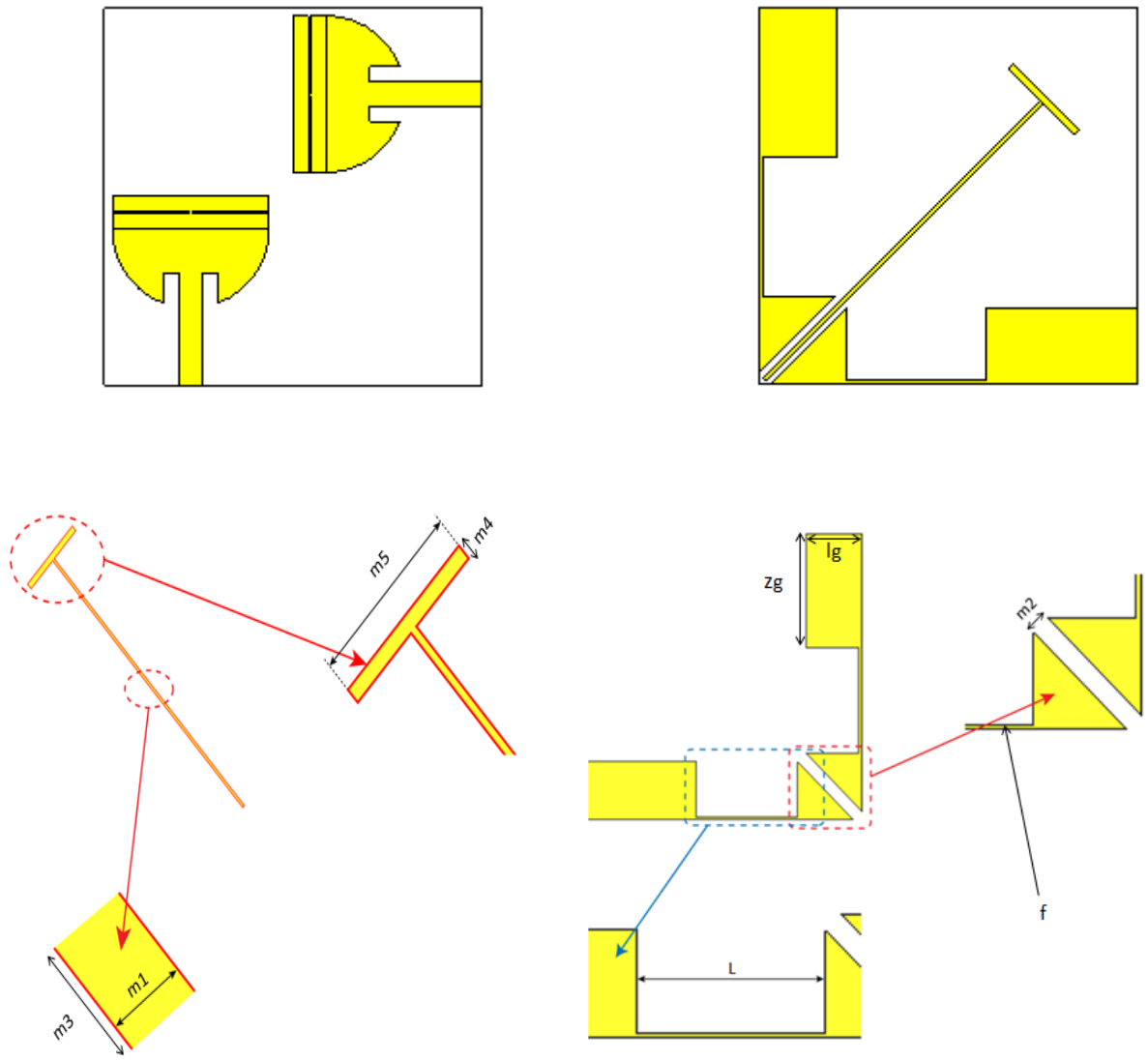

Figure 3. 1: The proposed pattern diversity structure.

Table 3. 1: Geometric dimensions of the proposed MIMO antenna.

Parameter	**R**	**X**	**Lf**	**Wf**	**Inl**	**Inw**	**Ls**	**Ws**	**Zg**	**L**
Value(mm)	10	2	10.02	3	4.15	2	9.8	0.3	20	17.8
Parameter	**Wg**	**Lg**	**Lsb**	**Wsb**	**M1**	**M2**	**M3**	**M4**	**M5**	**F**
Value(mm)	47.7	9.8	48	48	0.5	14	36	12	1	0.5

3.2.2 Design Evolution

The top side of the antenna is kept constant for all structures involved in the evolution study. The initial structure namely Antenna0 has a simple L-shaped ground with a slot introduced at the bottom corner of the ground plane as shown in Figure 3.2(a), with a length lg of 9.8 mm and width wg of 47.7 mm, respectively the slot dimensions are 13.85mm in length and 2 mm in width, the simulated results of S_{11} and S_{21} are shown in Figure 3.3 and represented by the green curves.It is clearly shown that the transmition exists while the isolation does not exist for all the 2.9-4.1 GHz band since the response is greater than -20dB.

To improve the isolation, Antenna1 is designed as shown in Figure 3.2(b) which is the result of cutting two rectangular shaped polygons from Antenna0 ground plane. Hence a rectangular open slot is created with dimensions $ls\ x\ ws = 17.77\,mm \times 9.88\,mm$. The design is simulated and the resulted S_{11}, S_{21} are represented in Figure 3.3 with the blue curves. It is clear that the isolation is considerably improved over the first operating frequency band 2.9-4.1 GHz and the antenna matching is also improved. It is worth to mention that only the first operating band will be considered in the reminder of this chapter.

By adding a simple rectangular stub to Antenna1, as shown in Figure 3.2(c), Antenna2 is designed. The length and the width of the stub are respectively 36 mm and 0.5 mm. The simulated S_{11} and S_{21} are presented with black curves in Figure 3.3. It is clear from the figure that both reflection and isolation coefficients are improved.

The final structure namely Antenna3 is shown in Figure 3.2(d). It is designed by attaching orthogonally another rectangular stub of 12 mm length and 1 mm width to the first stub, the resulted stub has a T-shaped geometry. The simulated S_{11} and S_{21} are presented, in red/orange color in Figure 3.3. It is noticed that the reflection coefficient is drastically improved especially at the resonance frequency of 3.75 GHz with a level of -60dB. Moreover, better isolation is obtained with S_{21} less than -20dB over a frequency band extending from 3.2 GHz to 4.1 GHz.

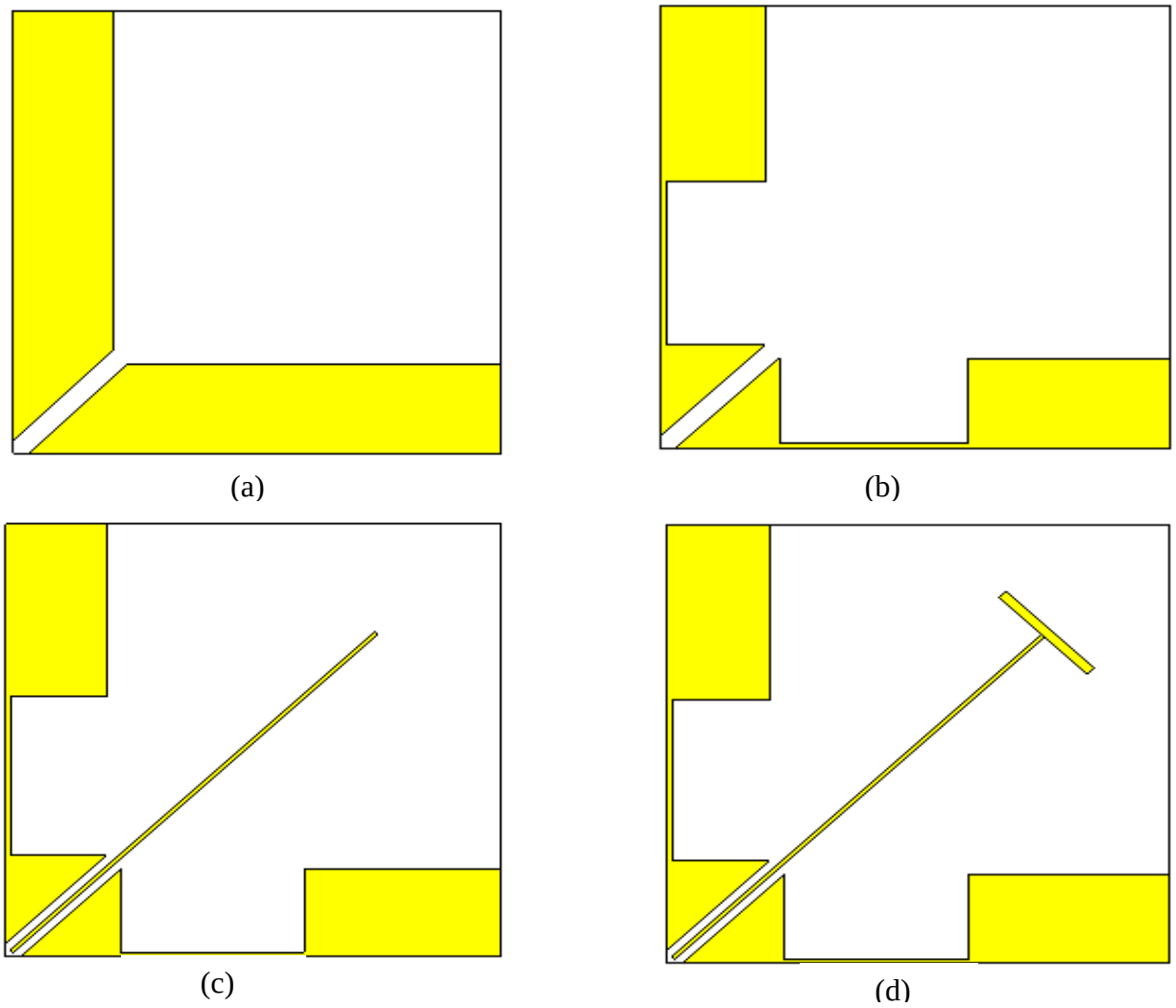

Figure 3. 2: Design evolution of (a) Antenna0 (b) Antenna1 (c) Antenna2 (d) Antenna3.

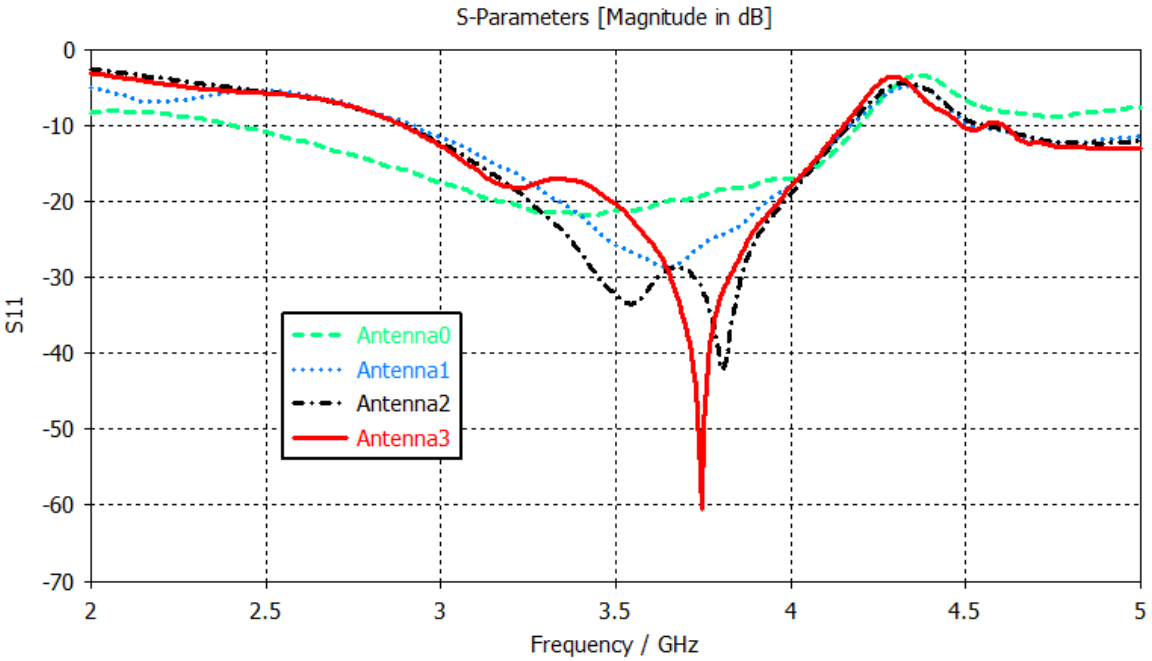

Figure 3. 3(a): Simulated return loss for various antennas involved in the design evolution.

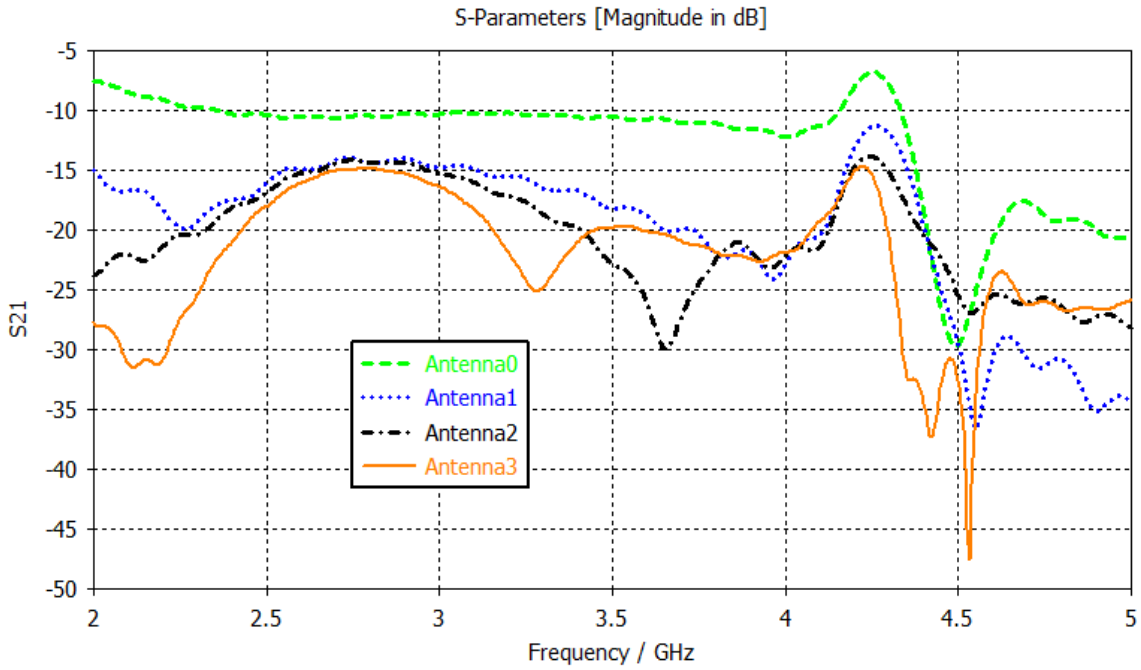

Figure 3. 3(b): Simulated isolation for various antennas involved in the design evolution.

3.2.3 Parametric Study

To understand isolation mechanism of the proposed structure, a parametric study is carry out. The simulations are done by changing one parameter at a time while keeping the remaining parameters unchanged.

The main goal of this part is designing the MIMO antenna for the optimum value of S_{21} to avoid coupling of the antennas.

3.2.3.a Effect of The First Stub Width (m1) on S_{21}

The effect of the stub width on S_{21} is shown in Figure 3.4. It is noticed from the obtained results that by increasing the stub length from 0.5 to 2 mm, the isolation improves in the frequency band 3.5-4.0 GHz while it deteriorates in the frequency band 3.2-3.5GHz. Best isolation is obtained for m1=0.5 mm since the S_{21} level is less than -20dB over the frequency band extending from 3.2 to 4.1 GHz.

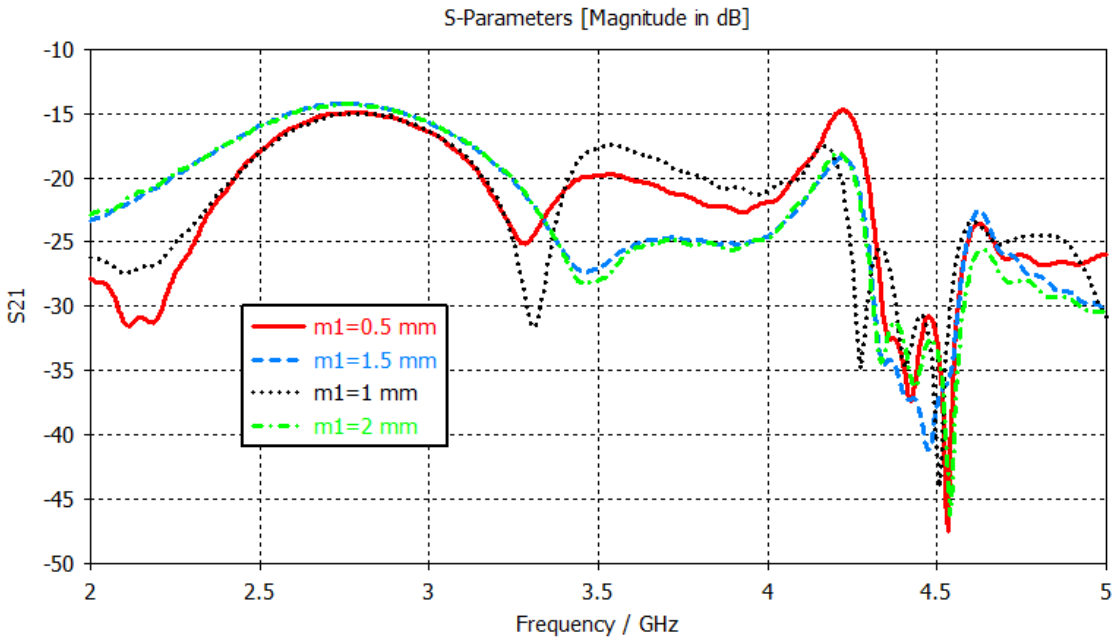

Figure 3. 4: Effect of m1 variation on S_{21}.

3.2.3.b Effect of First Stub Length (m3) on S_{21}

Figure 3.5 shows the simulated S_{21} for different values of m3. It is clearly seen that the isolation is slightly affected by the stub length m3 for the considered values 35, 36 and 37 mm. For m3=36 mm, the isolation is less than -20dB over a frequency band 3.2-4.1 GHz. Hence, the considered value of m3 is 36mm.

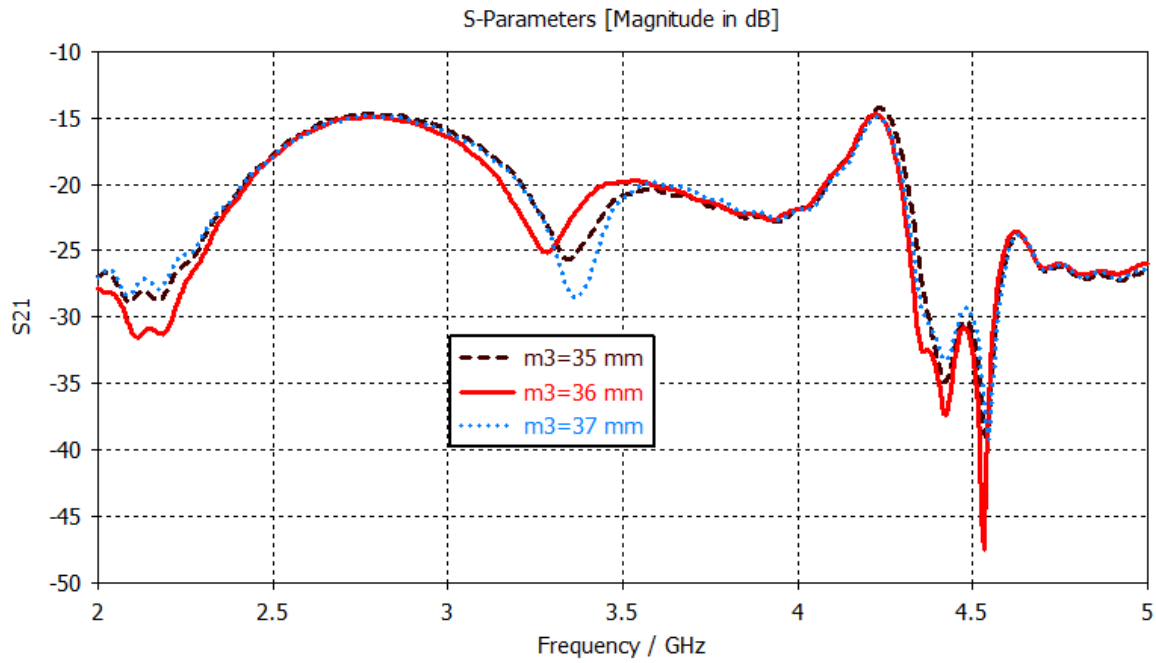

Figure 3. 5: Effect of m3 variation on S_{21}.

Effect of Second Stub Length (m4) on S_{21}

Figure 3.6 illustrates the simulated S_{21} for various values of m4.It noticeable From the Figure that the isolation is strongly affected by m4. It is also seen that the isolation is less than -20dB over the frequency band extending from 3.2 to 4.1 GHz for m4=12 mm.

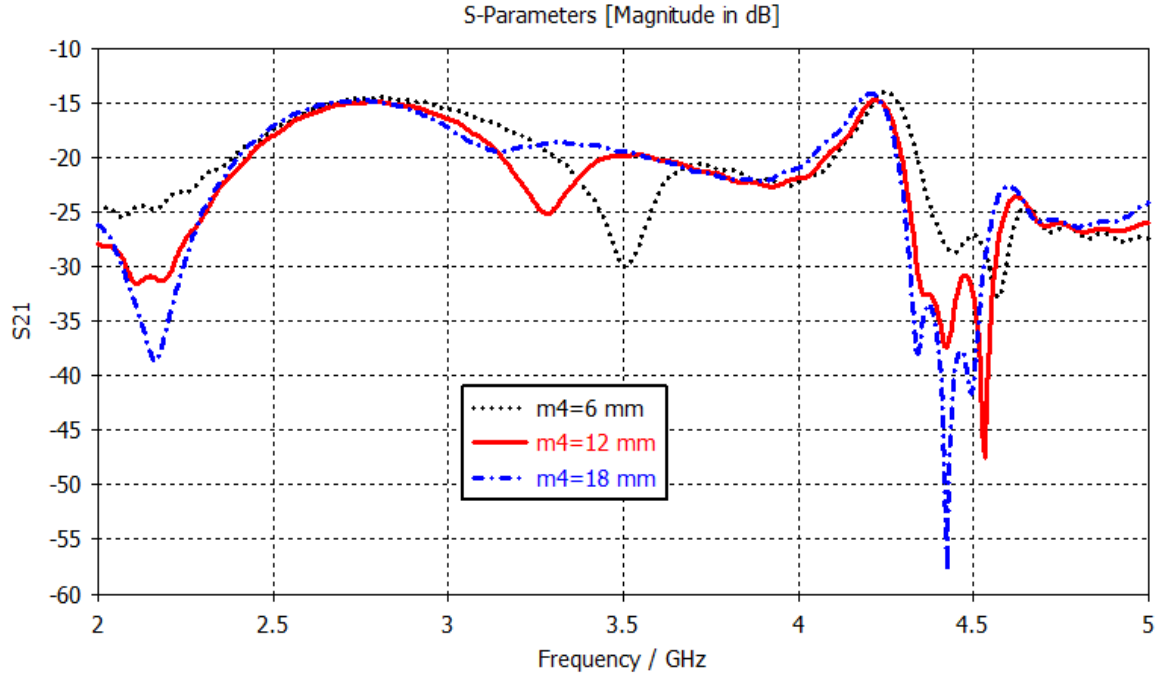

Figure 3. 6: Effect of m4 variation on S_{21}.

3.2.3.d Effect of Second Stub Width (m5) on S_{21}

The effect of varying m5 on the transmission coefficient S_{21} is depicted in Figure 3.7. It can be seen that by increasing the value of m5 from 0.5 to 1.0 mm by a step of 0.5 mm, a similar simulated isolations are obtained, while S_{21} is significantly affected when m5 equals 1.5 and 2 mm. Hence the considered value of m5 is 0.5 mm.

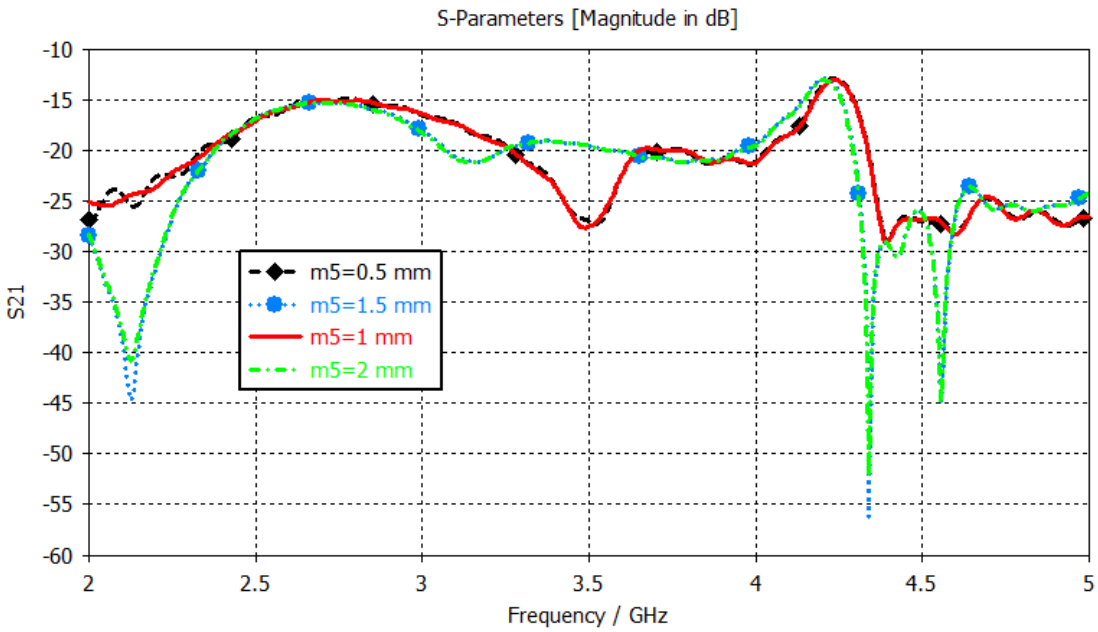

Figure 3. 7: Effect of m5 variation on S_{21}.

3.2.4 Current Distribution

The simulated current distribution for the proposed MIMO antenna at the resonant frequency of 3.75 GHz is shown in Figure 3.8. It is clear that for antenna one (vertical) the current is large at the feedline and is mainly concentrated on the central and lower parts of the semicircular patch as well as on two boundaries of the slots, while it is very weak on the patch corners. For antenna two (horizontal) there is no current flow which indicates the good isolation between the two elements. Moreover, the current is largely concentrated on the T-shaped stub. Hence, the current flowing from port 1 to port 2 is offset by the ground stub which reduces mutual coupling between antenna elements.

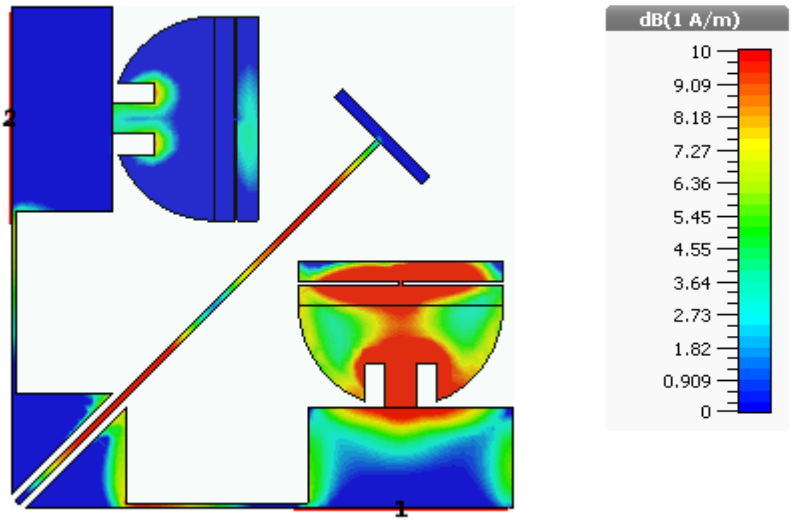

Figure 3. 8: Simulated current distribution on the pattern diversity structure

3.2.5 Radiation Pattern

The simulated 3D radiation pattern at 3.75 GHZ is presented in Figure 3.9. The E-Plane and H-plane radiation patterns are presented in Figure 3.10. It can be observed from the far-field radiation patterns that the radiation pattern is omnidirectional in H-plane as shown in Figure 3.10(b) and bidirectional in E-plane as illustrated in Figure 3.10(a). It is also seen that the peak simulated gain is of 3.57dB.

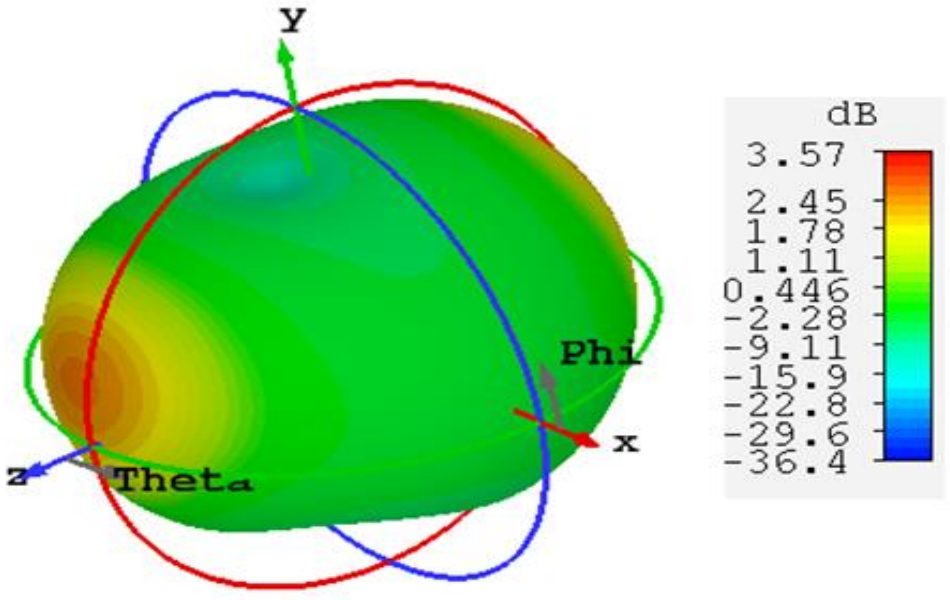

Figure 3. 9: 3D Simulated radiation pattern at 3.75 GHz.

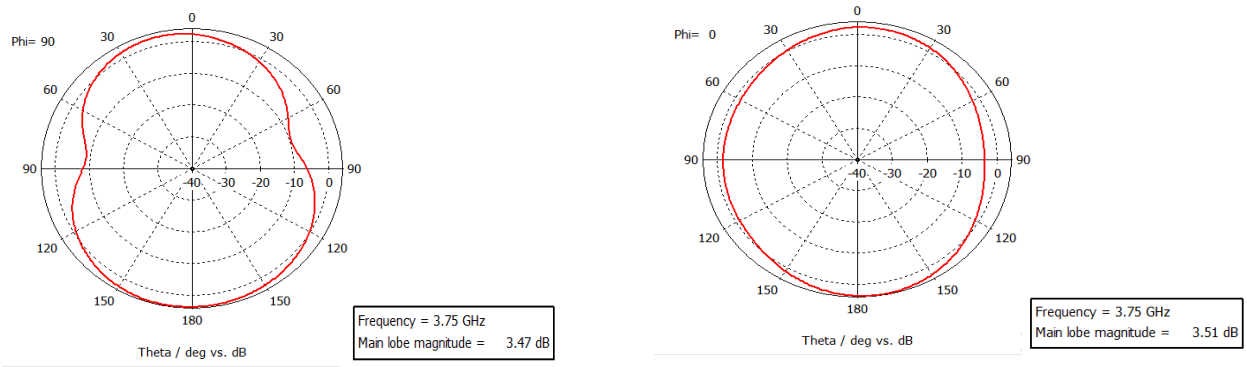

(a) (b)

Figure 3. 10: 2D simulated radiation pattern (a) E-plane and (b) H-plane.

3.3 Spatial Diversity Configuration

3.3.1 Structure Geometry Description

The structure consists of two identical cup-shaped antenna elements placed symmetrically in mirror configuration on a substrate (FR4) with ε_r= 4.3, loss tangent 0.017 with width of 1.6 mm. the distance between the radiators is adjusted till the decoupling is less than -22 dB in the frequency range of 3 GHz-3.75 GHz and it is set to be 2 mm. A vertical stub is introduced in the ground plane to achieve better isolation. Moreover, two open ended slots etched in both sides of the stub to further enhance the decoupling process. The given configuration is illustrated in figure 3.11 and its dimensions are given in table 3.2.

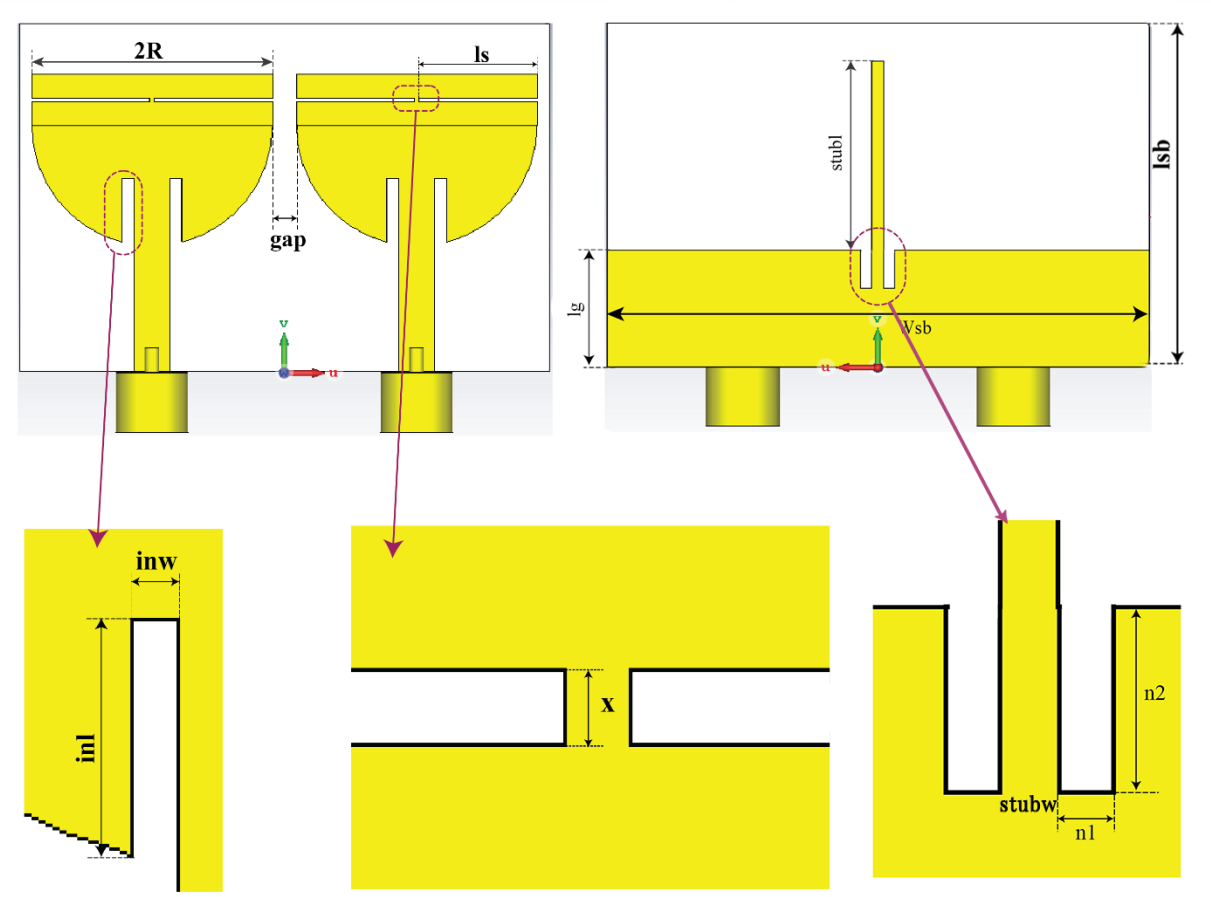

Figure 3. 11: Schematics of the proposed MIMO antenna.

Table 3. 2: Geometrical parameters of the proposed structure

Parameter	R	Ls	Lf	inw	inl	x	Lg	stubl	stubw	gap	n1	n2	Wsb	Lsb
Value	10	9.8	10.7	1	5.8	2	9.8	12	0.5	2	0.5	4	44	29

The proposed structure dimensions are given in table 3.2. The simulation and analyses of the proposed design is carried out by using the commercial electromagnetic simulation software CST. The simulated reflection coefficient S_{11} and transmission coefficient S_{21} are shown in Figure 3.12 and 3.13 respectively

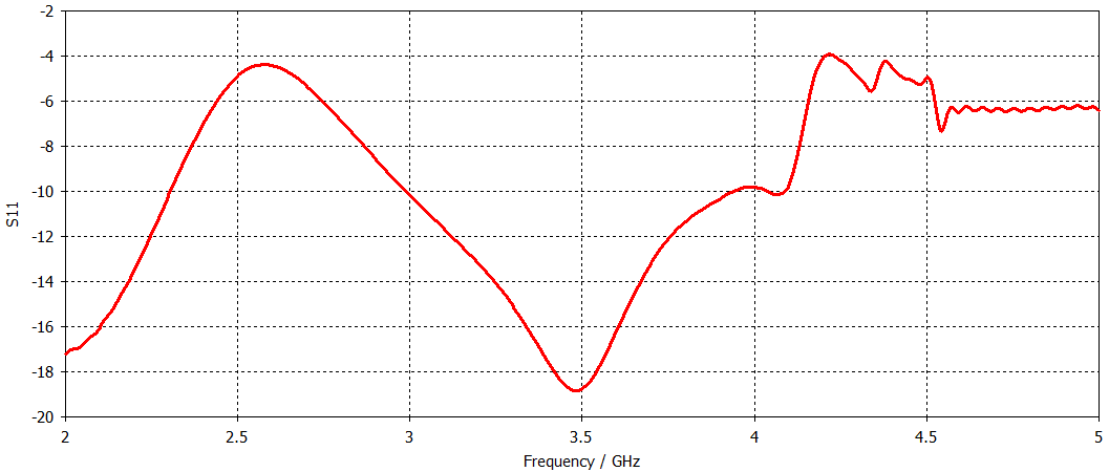

Figure 3. 12: The return loss for spatial diversity configuration.

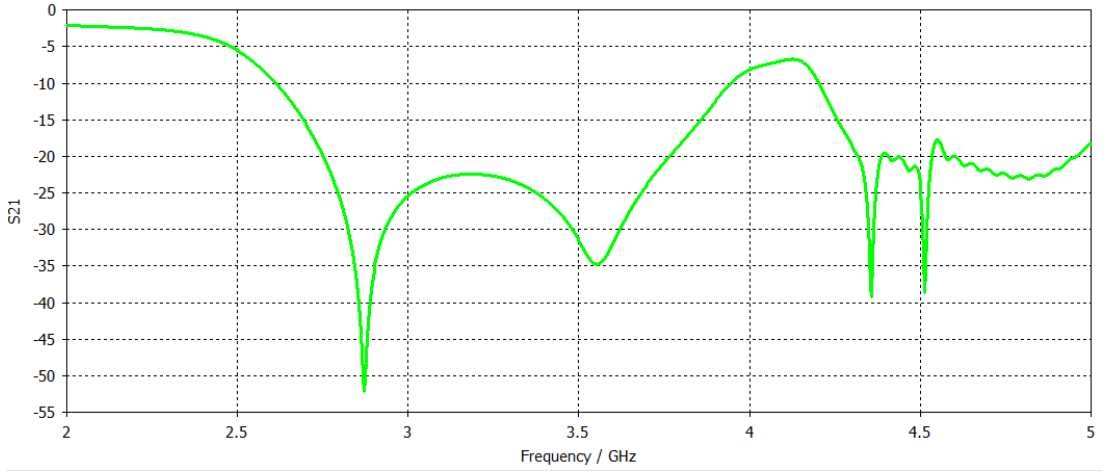

Figure 3. 13: The transmission coefficient for spatial diversity configuration.

We can see from the obtained results that the antenna is operating in the frequency band extending from 3 to 4 GHz centered at 3.5 GHz. To achieve better isolation, the technique used is the insertion of a vertical stub in the common ground plane Moreover, to enhance the reduction of mutual coupling between the monopole radiators, slots are etched out in the ground plane. S_{21} level in the frequency range of 3 GHz to 3.75 GHz is below -22 dB which can be taken as a good result for the isolation parameter in the given frequency range.

3.3.2 Stub Effect

One of the challenges the designer can face during the construction of a MIMO antenna system is mutual coupling. Introducing stubs can be used to enhance the decoupling between the MIMO radiating elements and hence reduce the spacing between them. However, these stubs need suitable dimensions in order to perform correctly and give better results under a

certain frequency range. A parametric study is proposed to study the effect of stub dimensions on the antenna performances. To start, we will evaluate our design without the stub and see the effect of its presence in the system. Figure 3.14 shows the ground plane without stub and Figure 3.15 shows the corresponding simulated transmission coefficient.

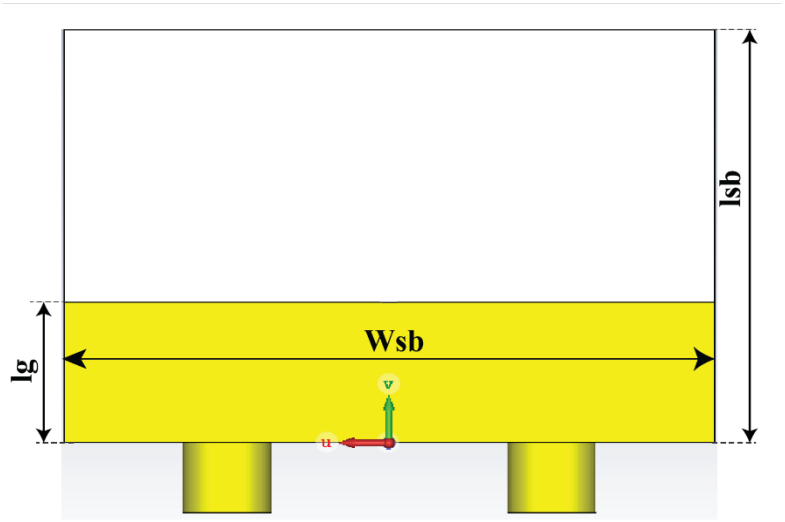

Figure 3. 14: Ground plane without stub.

We can see from the obtained results that the absence of the stub caused a noticeable deterioration of the isolation. S_{21} level is above -20dB along the whole range of frequencies. From these results, we can conclude that the stub improves significantly the isolation between the antenna elements especially in the band from 3 GHz to 3.75 GHz.

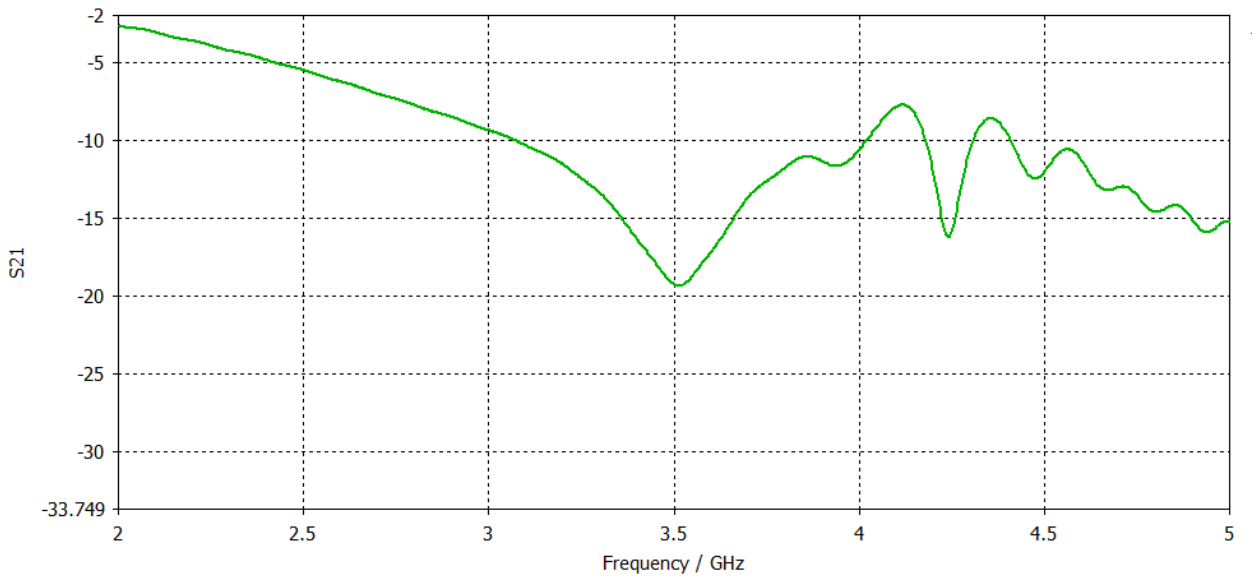

Figure 3. 15: The simulated S_{21} without the vertical stub.

3.3.2.a Effect of Stub Length on the Isolation

In following sections, the effect of the inserted vertical stub, in the ground plane of the proposed MIMO antenna, will be investigated. The simulated isolations for different values of the stub length are illustrated in the Figure 3.16. It can be seen from the obtained results that the isolation between element 1 and 2 is affected by the stub length. For stub length of 12 mm, the isolation is less than -22dB over the frequency range extending from 3 GHz to 3.75 GHz. Therefore, the length of the stub is taken as stubl=12 mm.

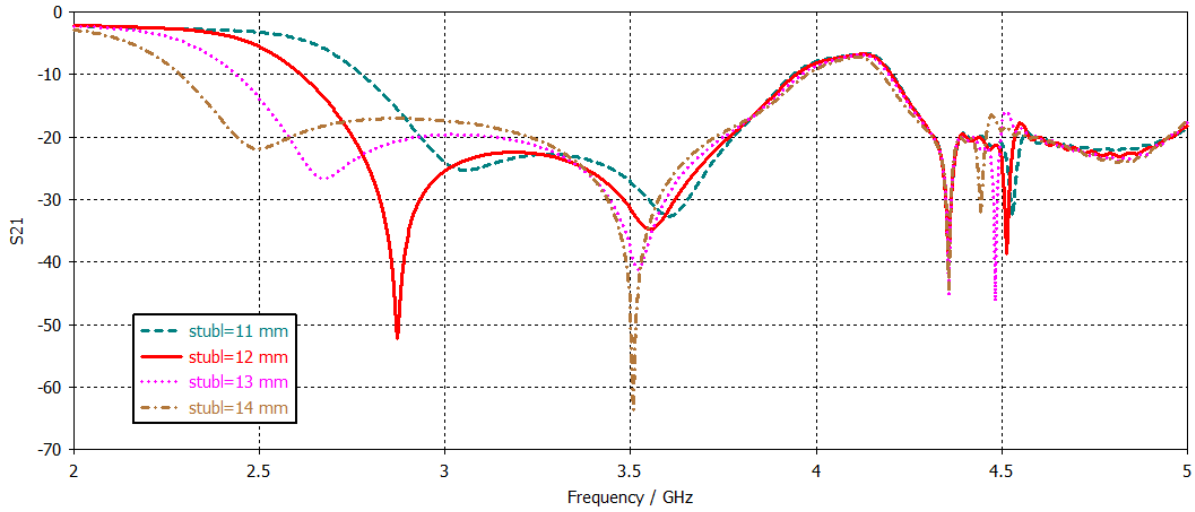

Figure 3. 16: Stub length effect on S_{21}.

3.3.2.b Effect of Stub Width on the Isolation

The effect of varying the stub width on the isolation/decoupling is illustrated in Figure 3.17. It can be seen that the isolation between the elements 1 and 2 deteriorates when the stub width is increased from 0.5 to 1.5 mm. The isolation is less than -22dB over the frequency range extending from 3 GHz to 3.75 GHz. Consequently, the considered value of stubw is 0.5 mm.

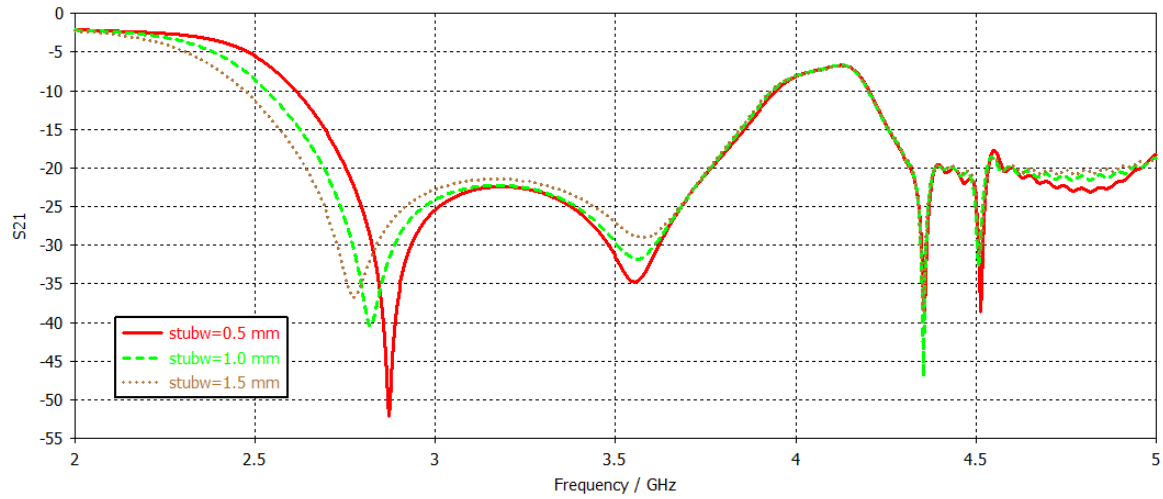

Figure 3. 17: Stub width effect on S_{21}.

3.3.2.c Effect of Open-Ended Slots on the isolation

We have seen previously that the variation in the stub geometrical parameters led us to obtain better isolation level. In this section the effect of open ended slots etched from the MIMO antenna ground plane is studied. The configuration of the introduced slots is illustrated in the Figure 3.18

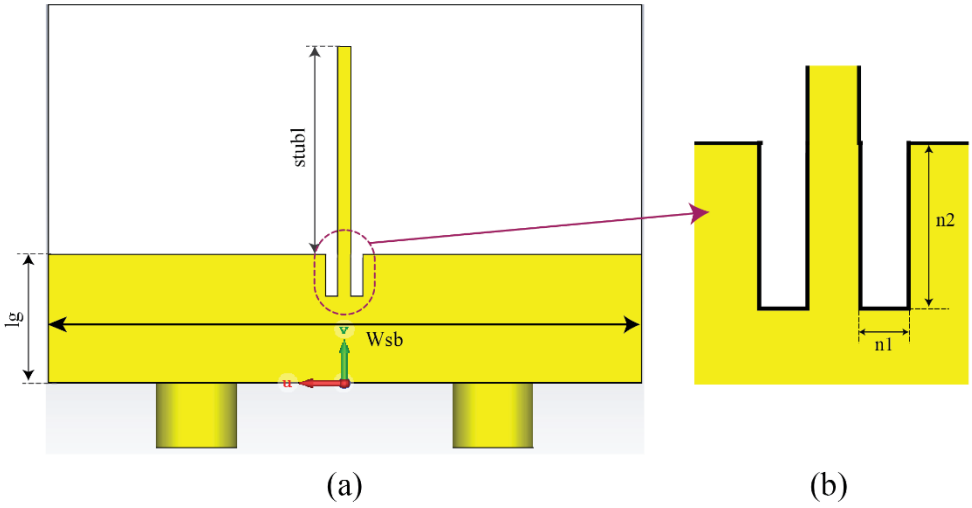

Figure 3. 18: Ground plane with stub and etched slots

3.3.2.d Effect of Changing n1 (slot width)

In this part, the open slots width effect on S_{21} will be investigated. The optimized geometrical parameters found before are kept unchanged. Figure 3.19 below depicts the variation of S_{21} for various values of n1. It can be seen from the obtained results that by increasing the slots width from 0.5 mm to 1mm, the S_{21} degrades especially in the frequency range from 3 GHz to 3.25 GHz. Better result in term of isolation is achieved for n1=0.5 mm.

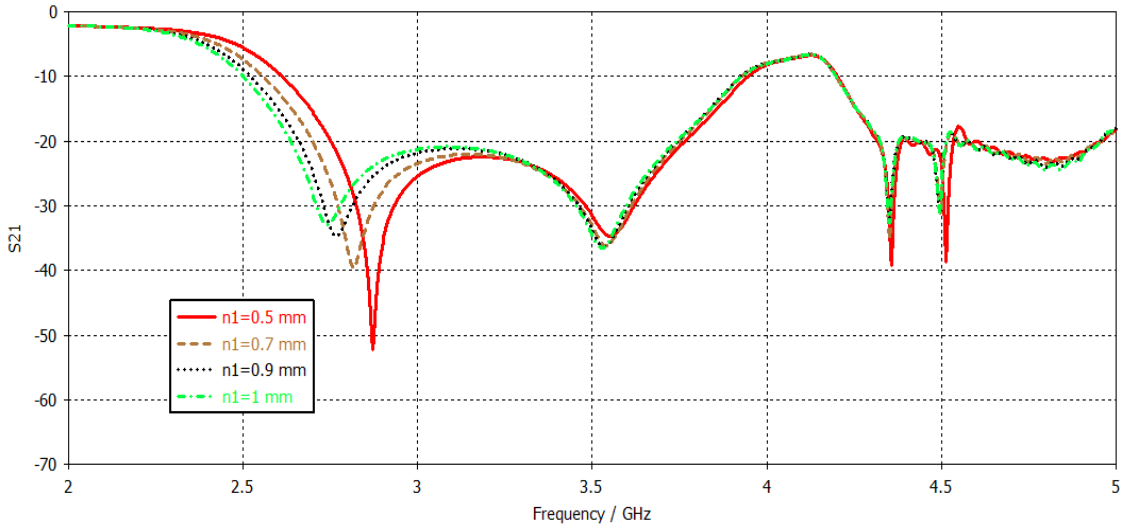

Figure 3. 19: Slot width effect on S_{21}

3.3.2.e Effect of Changing n2 (slot length)

The effect of changing the inserted slots length on the isolation is illustrated in Figure 3.20. The simulation is performed by varying only one parameter, which is n2, and keeping the remaining geometrical parameters constant. From the figure, by increasing n2 from 4 mm to 6 mm by a step of 1mm, the isolation is less than -22dB over the frequency range extending from 3 GHz to 3.75 GHz with a higher level for n2=4 mm.

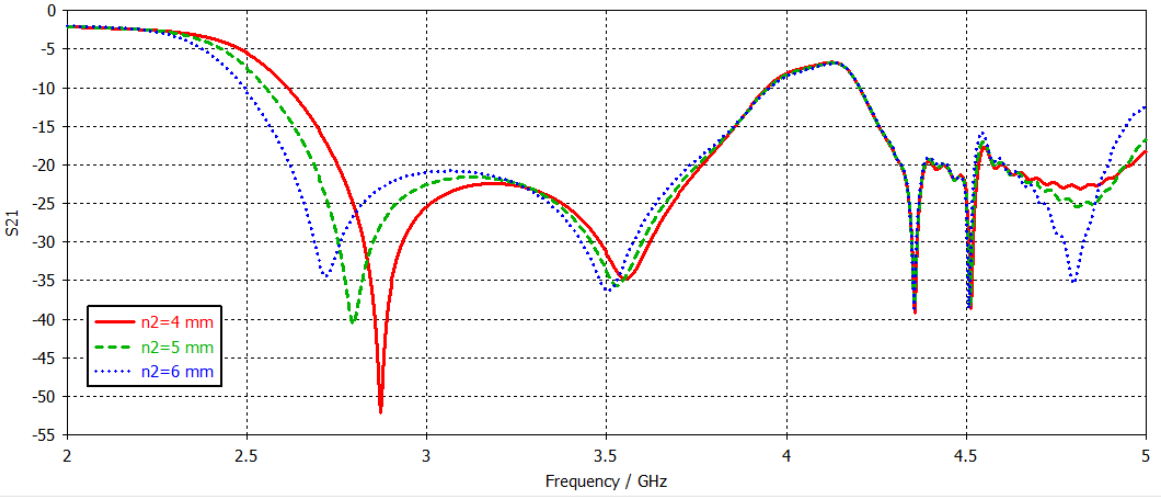

Figure 3. 20: Effect of slot length on S_{21}

3.3.3 The Current Distribution

The simulated current distribution at the resonant frequency of 3.5 GHz is depicted in Figure 3.21. The single port 1 is excited, maximum of the current is observed on feedline, radiation patch, and decoupling stub. By comparing these two radiating elements, we can

conclude that the introduced stub produce resonance to trap the coupling current, so that the induced current is decreased in the adjacent antenna element. Thus, high isolation is efficiently realized.

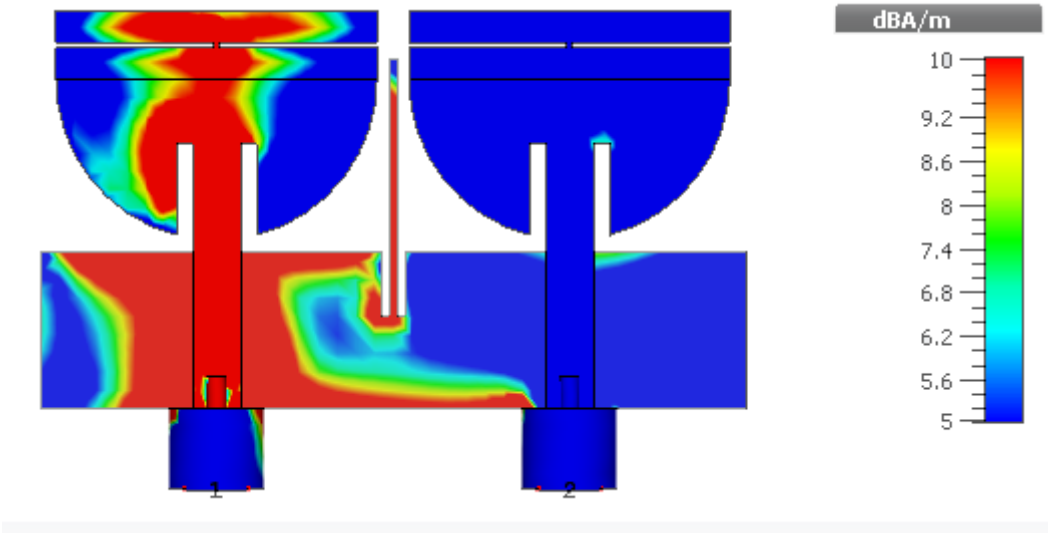

Figure 3. 21: The simulated current distribution at 3.5 GHz.

3.3.4 Radiation Pattern

The simulated 3D radiation pattern at 3.5 GHz is presented in Figure 3.22. The E-Plane and H-plane radiation patterns are also illustrated in Figure 3.23. It can be observed from the far-field radiation patterns that the MIMO antenna exhibits an Omni-directional at the resonant frequency in both E and H planes. Furthermore, it can be observed that the peak simulated gain is 2.78dB.

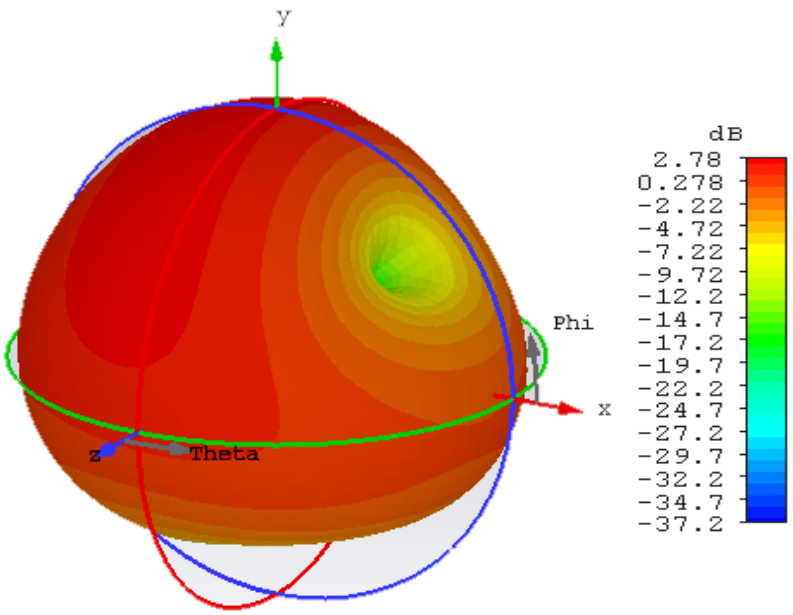

Figure 3. 22: 3D simulated radiation pattern at 3.5 GHz.

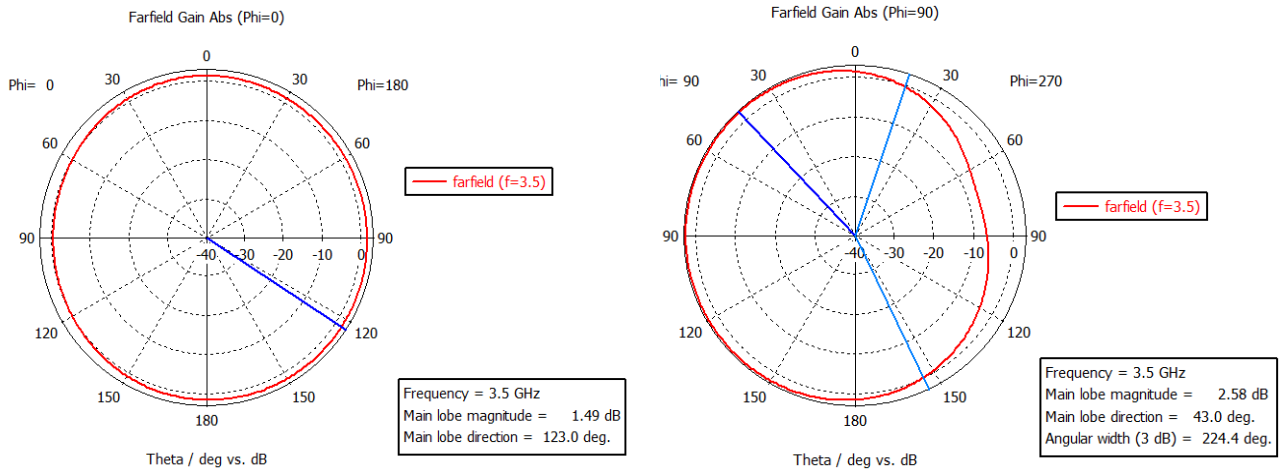

(a) (b)

Figure 3. 23: 2D simulated radiation pattern (a)E-plane and (b) H-plane.

3.4 Experimental Results

To validate the technical proposal, the proposed MIMO antennas were fabricated and tested. Figure 3.24 and Figure 3.25 show the photograph of the fabricated prototypes of the proposed MIMO antennas. The fabricated structure performances were measured using a vector network analyzer (VNA) operating in the frequency band from 100 KHz to 20 GHz. The measurement setup for the pattern diversity configuration is shown in Figure 3.26.

Figure 3.27 shows measured and simulated return losses and isolations for pattern diversity configuration. It is observed that the measured and simulated results are in acceptable agreement. The measured -10dB impedance bandwidth is 1.5 GHz (2.5-4 GHz) covering largely the 3.5 GHz WiMAX band. In addition, the measured S_{21} is less than -20dB throughout the operating bandwidth. The slight deviation between the measured and simulated results is basically due to the manufacturing tolerances, the uncertainty on the thickness and dielectric relative constant of the substrate added to the SMA connectors quality.

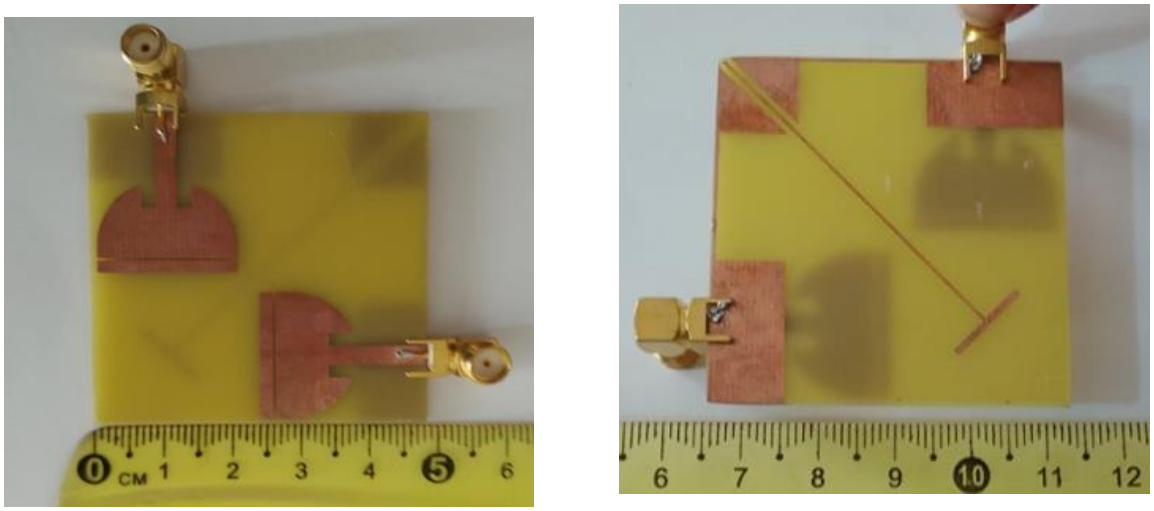

(a) (b)

Figure 3. 24: Photograph of pattern diversity configuration (a) front view (b) back view.

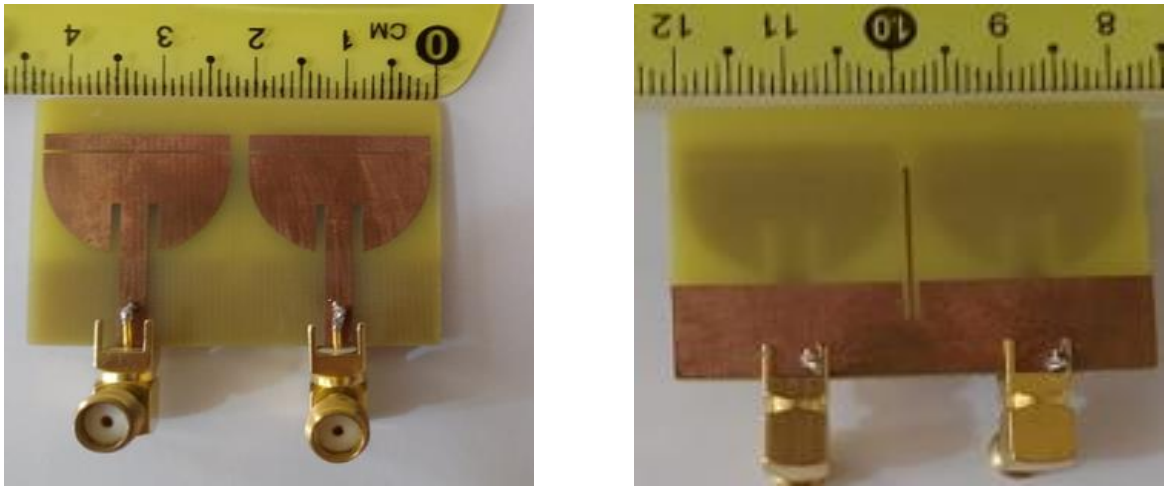

(a) (b)

Figure 3. 25: Photograph of the spatial diversity configuration (a) front view(b) back view.

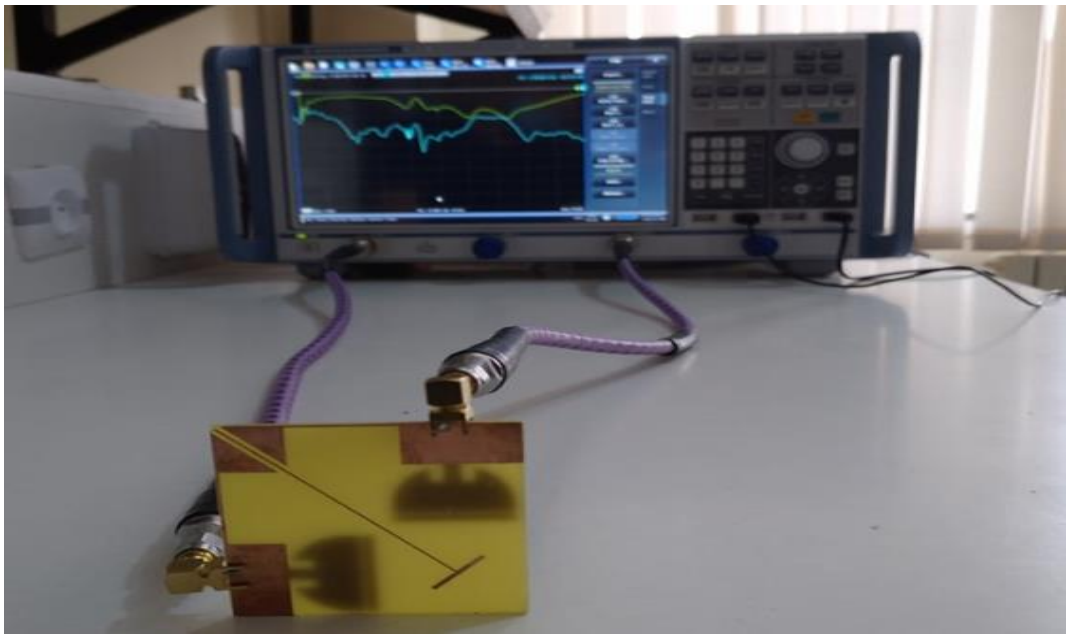

Figure 3. 26: Measurement setup.

Figure 3.28 shows measured and simulated return losses and isolations for spatial diversity configuration. It can be clearly seen that the measured and simulated results are in good agreement. The measured -10dB impedance bandwidth is 1.25 GHz (2.75-4.0 GHz) covering widely the 3.5 GHz WiMAX band. Furthermore, the measured S_{21} is less than -20dB over the operating bandwidth.

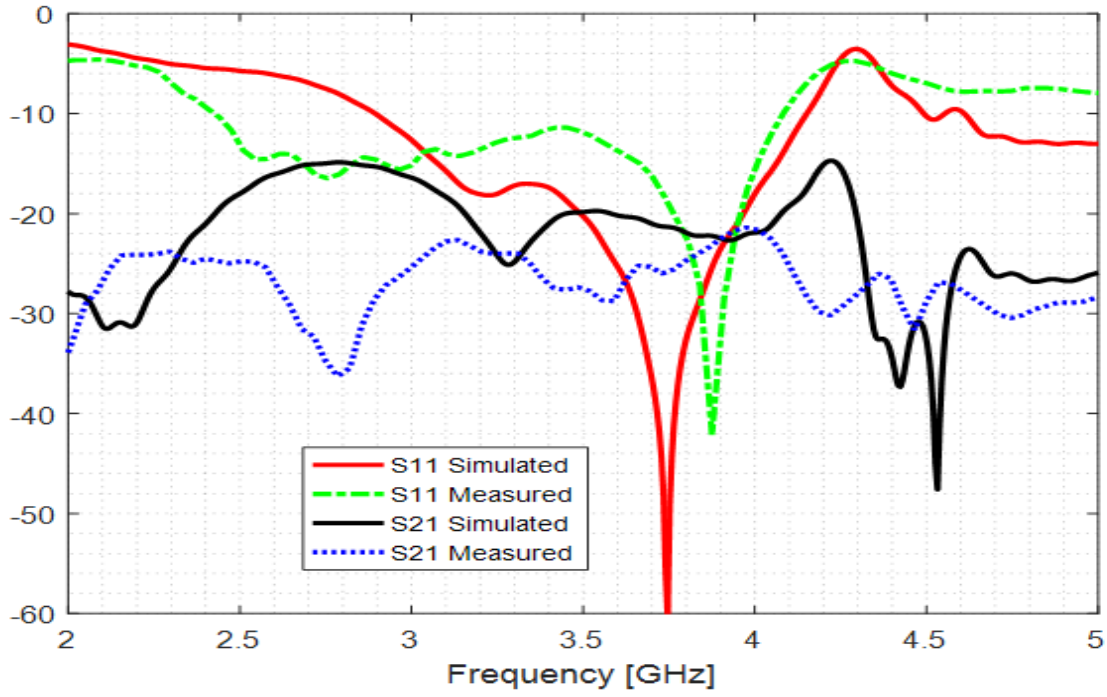

Figure 3. 27: Measured and simulated $S_{11}$and S_{21} parameters of pattern diversity configuration

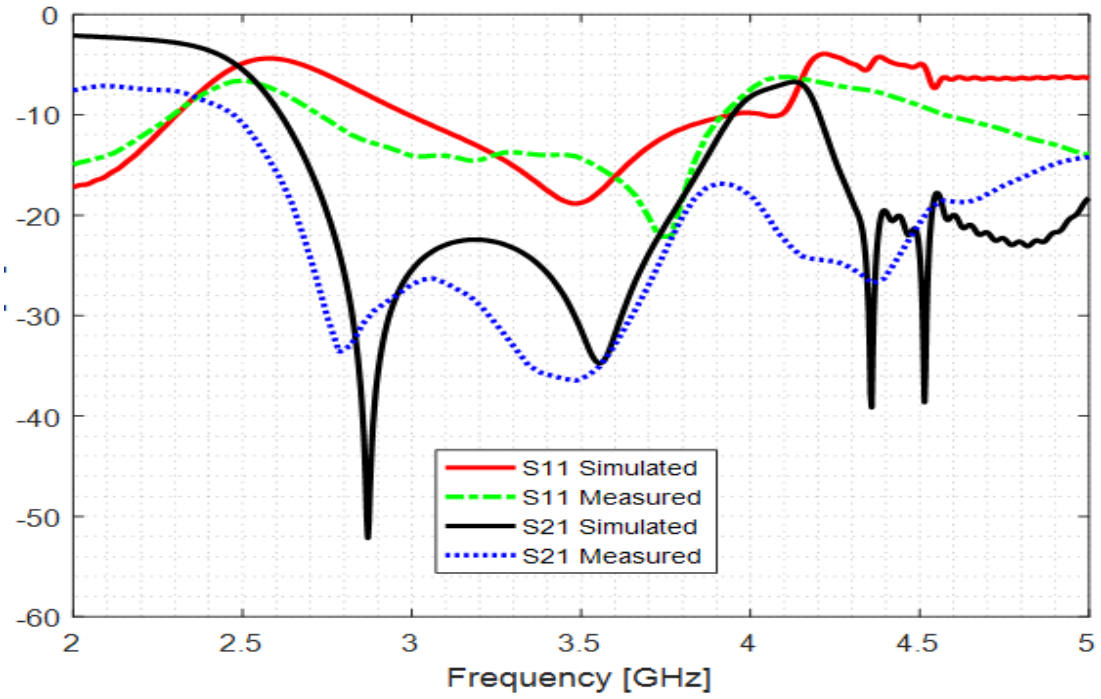

Figure 3. 28: Measured and simulated S_{11} and S_{21} parameters of spatial diversity configuration.

3.5 Conclusion

In this chapter the design and analysis of spatial and pattern diversity configuration MIMO antennas have been presented. The slotted cup-shaped antenna element has been designed to cover the 3.5GHz WiMAX application. The high isolation in the proposed pattern diversity configuration has been achieved by loading the antenna ground plane with two slots and inserting a T-shaped stub. The resulted structure has compact dimensions of 48 x 48 mm^2 and exhibit an omnidirectional radiation pattern with a simulated peak gain of 3.57dB. Using same antenna elements placed side-by-side with an inters pacing of 2 mm, a second MIMO configuration, spatial diversity, has been designed. The structure is compact with a footprint of

29 x 44mm^2. A high isolation of less than -22dB over an operating band extending from 3 to 4 GHz has been achieved by inserting a rectangular stub in the ground plane and etching two open-ended slots in adequate positions. The proposed MIMO antennas have been prototyped and tested and a good agreement has been observed between the simulated and measured return losses.

General Conclusion

In this work the design of two-element spatial and pattern diversity configurations of slot-loaded cup-shaped monopole antenna have been proposed. The antenna element has been designed to operate in the 3.5 GHz frequency band allotted to the WiMAX application.

Firstly, the antenna element has been designed to operate in the frequency band covering the intended application. An evolution study to produce the final element geometry has been caried out with help of a full wave based simulator CST. The final structure has a cup-shaped patch load with two symmetrical open-ended slots. The proposed structure operates at the frequency band extending from 3 GHz to 4 GHz and has an omnidirectional radiation pattern which makes it suitable to be used in wireless applications.

Then, two elements have been used to design two different antennas for MIMO application. The proposed structures are pattern and diversity configurations. The high isolation in the proposed pattern diversity configuration has been achieved by inserting a T-shaped stub and etching two rectangular slots in antenna ground plane. The resulted structure has compact dimensions of 48x48mm^2 and exhibits an omnidirectional radiation pattern with a simulated peak gain of 3.57dB.

Finally, in spatial diversity configuration, two antenna elements placed in side-by-side configuration with an inter element spacing of 2 mm has been designed. The structure is compact with a footprint of 29x44 mm2. A high isolation of less than -22dB over an operating band extending from 3 GHz to 4 GHz has been achieved by inserting a rectangular stub in the antenna ground plane and etching two open-ended slots in the vicinity of the inserted stub. The resulted structure has an omnidirectional radiation pattern with a simulated peak gain of 2.78dB.

The proposed cup-shaped MIMO antennas have been prototyped and tested and a good agreement has been observed between the simulated and measured scattering parameters S_{11} and S_{21}.

REFERENCES

References

[1] Introduction to Wireless and Telecommunication, 23 JUIN 2017. [online].

[2] Foschini GJ and Gang MJ "On limits of wireless communications in a fading environment when using multiple antennas". Wireless personal communication,6, 311-335, 1998.

[3] Tang Z, Wu X, Zhan J, Hu S, Xi Z and Liu Y (2019) Compact UWB-MIMO antenna with high isolation and triple-band notched charachteristics. IEEE access, 7,19856-19865.

[4] H. Howe, "Microwave integrated circuits - An Historical Prospective", vol. Vol 32, September,1984, pp. 991-996.

[5] Lo, Y. T. D. Solomon, and W. F. Richards "Theory & Experiments on Microstrip Patch antenna", 1997, pp. 137-145.

[6] C. A. Balanis, Antenna Theory, Analysis and Design, New york: John Wiley & Sons, 2005.

[7] T. S. Bird,2009. "Definition and misuse of return loss". IEEE Antennas and Propagation Magazine, 2009, pp. 166-167..

[8] D. M. Pozar, "Microwave Engineering", Fourth edition, 1998 by John & Wiley Sons.

[9] D.G.Fang, "Antenna Theory and Microstrip Antennas", 2010.

[10] Khan, V. Harsha Ram Keerthi and Dr. Habibullah, «"Design of C-Band Microstrip Patch Antenna for Radar Applications Using IE3D"» .pp. 49-58, Mars-April 2013.

[11] H. F. Pues and A. R. Van De Capelle,"An impedance Matching Technique for Increasing the Bandwidth of Microstrip Antennas", November 1989,pp. 1345-1354.

[12] K. F. Lee, K. M. Luk "Microstrip Patch Antennas", Imperical College Press, 2011.

[13] Biglieri E, Calderbank R "MIMO Wireless communications", Cambridge University Press, 2007.

[14] Jankiraman M. Space-Time codes and MIMO Systems, London , UK: Artech House, Inc,

2004.

[15] M.V., Kartikeyan Leeladhar Malviya Rajib Kumar Panigrahi"MIMO Antennas for wireless communication theory and design", 2021.

[16] Franco De Flaviis, Louis Jofre, Jordi Romeu, Alfred Grau. "Multi-Antenna Systems for MIMO Communications". By Morgan and Claypool, 2008.

[17] S. T. Harsh Verdhan Singh, «Compact UWB MIMO antenna with cross-shaped unconnected ground stub using characteristic mode,» International Institute of Information Technology, Naya Raipur, Chhattisgarh, India, 2018.